

SurgeryV2: Bridging the Gap Between Model Merging and Multi-Task Learning with Deep Representation Surgery

Enneng Yang, Li Shen, Zhenyi Wang, Guibing Guo, Xingwei Wang, Xiaochun Cao,
Jie Zhang, and Dacheng Tao, *Fellow, IEEE*

arXiv:2410.14389v1 [cs.LG] 18 Oct 2024

Abstract—Model merging-based multitask learning (MTL) offers a promising approach for performing MTL by merging multiple expert models without requiring access to raw training data. However, in this paper, we examine the merged model’s representation distribution and uncover a critical issue of “representation bias”. This bias arises from a significant distribution gap between the representations of the merged and expert models, leading to the suboptimal performance of the merged MTL model. To address this challenge, we first propose a representation surgery solution called *Surgery*. *Surgery* is a lightweight, task-specific module that aligns the final layer representations of the merged model with those of the expert models, effectively alleviating bias and improving the merged model’s performance. Despite these improvements, a performance gap remains compared to the traditional MTL method. Further analysis reveals that representation bias phenomena exist at each layer of the merged model, and aligning representations only in the last layer is insufficient for fully reducing systemic bias because biases introduced at each layer can accumulate and interact in complex ways. To tackle this, we then propose a more comprehensive solution, deep representation surgery (also called *SurgeryV2*), which mitigates representation bias across all layers, and thus bridges the performance gap between model merging-based MTL and traditional MTL. Finally, we design an unsupervised optimization objective to optimize both the *Surgery* and *SurgeryV2* modules. Our experimental results show that incorporating these modules into state-of-the-art (SOTA) model merging schemes leads to significant performance gains. Notably, our *SurgeryV2* scheme reaches almost the same level as individual expert models or the traditional MTL model. The code is available at <https://github.com/EnnengYang/SurgeryV2>.

Index Terms—Multi-task Learning, Model Merging, Model Fusion, Machine Learning

I. INTRODUCTION

Multi-task learning (MTL) leverages a single model to predict multiple related tasks, thereby reducing parameter costs

This paper is an extended version of our previous work [1] presented at ICML 2024. In this extended version, we re-analyze the limitations of the original approach and propose a new scheme, *SurgeryV2*, which delivers improved performance, reduced data requirements, and faster training speed compared to the previous method.

Enneng Yang, Guibing Guo, and Xingwei Wang are with Northeastern University, China. E-mail: ennengyang@stumail.neu.edu.cn, guogb,wangxw}@swc.neu.edu.cn.

Li Shen and Xiaochun Cao are with School of Cyber Science and Technology, Shenzhen Campus of Sun Yat-sen University, Shenzhen 518107, China. E-mail: mathshenli@gmail.com, caoxiaochun@mail.sysu.edu.cn.

Zhenyi Wang is with the University of Maryland, USA. E-mail: wangzhenyineu@gmail.com.

Jie Zhang and Dacheng Tao are with Nanyang Technological University, Singapore. E-mail: zhangj@ntu.edu.sg, dacheng.tao@gmail.com.

and facilitating cross-task knowledge transfer [2, 3, 4, 5]. MTL has been extensively applied across various domains, including computer vision [6, 7, 8, 9, 10, 11], natural language processing [12, 13], recommendation systems [14, 15, 16] and speech recognition [17, 18]. However, the traditional MTL paradigm requires pre-collection of training data for all tasks and then collaboratively training an MTL model, which may lead to privacy leakage of valuable data and additional data management costs, particularly when dealing with large datasets or numerous tasks.

Recently, a novel approach known as “model merging” or “model fusion” [19, 20, 21, 22, 23, 24, 25, 26, 27, 28, 29, 30, 31, 32, 33] has emerged within the machine learning community, demonstrating promise in addressing these challenges. The goal of model merging is to directly merge multiple expert models that have been trained individually on various tasks, to perform MTL without accessing their raw training data. In other words, model merging relies solely on the trained model parameters for each task, eliminating the need for centralized management of MTL training data and joint training. This innovative approach significantly broadens the potential applications of MTL. Despite these advancements (§II), a notable performance gap persists between the most advanced model merging-based MTL methods [34, 35, 24, 21, 20, 21, 26] and traditional MTL or individual expert models. This gap motivates our investigation into the underlying issues of model merging and develops solutions to close this gap.

In this paper, we revisit several representative model merging schemes [34, 36, 21, 26] from the perspective of the representation distribution, identifying a common challenge: “representation bias” (§IV-A). Representation bias is defined as the gap between the representations extracted by the merged model and those extracted by the individual models. Recall that the primary goal of model merging is to create a unified model that retains the capabilities of all individual expert models. Therefore, to quantify the alignment between the merged model’s representations and those of the expert models, we introduce a novel metric and conduct extensive evaluations across eight tasks (e.g., SUN397 [37], Cars [38], etc.), three architectures (i.e., ViT-B/32, ViT-B/16, and ViT-L/14 [39]), and four representative model merging methods (i.e., Weight Averaging [34], Task Arithmetic [36], Ties-Merging [21], AdaMerging [26]). By examining the relationship between the representation bias of the merged model and its final MTL performance, we empirically demonstrate that representation

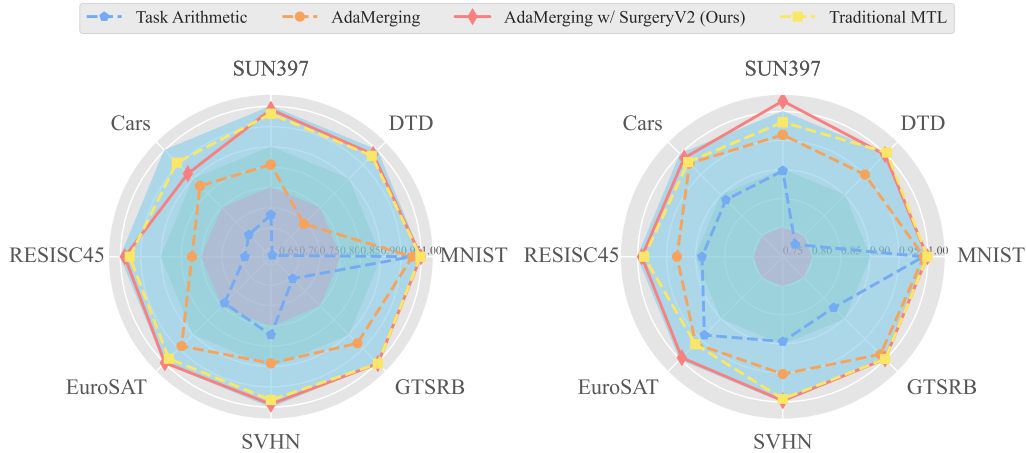


Fig. 1: The *SurgeryV2* scheme achieves performance comparable to traditional MTL when merging eight benchmark tasks and two architectures (left: ViT-B/32, right: ViT-L/14). We report the performance normalized with the individual expert model’s performance, which is denoted by the white circle of radius 1.

bias is a critical factor limiting the performance of the merged model. Consequently, reducing representation bias can achieve better model merging performance.

To solve the “representation bias” problem in model merging, we first propose a novel representation surgery solution (§IV-B), termed *Surgery*, which aligns the representation of the merged model at the *last layer* with the representation of the individual expert model at the *last layer*. Since raw training data are not available, we design an unsupervised surrogate objective to update parameters in the *Surgery* module. Notably, this approach achieves a new SOTA performance among existing model merging methods. However, there is still a relatively obvious representation bias after using the representation surgery scheme, and the MTL performance of the merged model is still far behind the traditional MTL method. This result prompted us to conduct a deeper analysis of the representation surgery method to further reduce representation bias and narrow the performance gap.

We carefully analyze the correlation between the capacity of the *Surgery* module and the degree of representation bias (§IV-C), finding that simply increasing the capacity can effectively reduce the bias and improve merging performance. However, beyond a certain threshold, further increasing capacity no longer yields benefits. Additionally, our layer-by-layer analysis reveals that representation bias exists at each layer of the merged model, with the bias magnitude increasing monotonically with the depth of the layer in the merged model. In summary, representation bias exists at every layer of the merged model, and addressing only the last layer—even with a substantial capacity—fails to fully resolve systemic representation bias. This is because the biases introduced at each layer can accumulate and interact in complex ways. To overcome this limitation, we then propose a deep representation surgery solution (§IV-D), abbreviated as *SurgeryV2*, which effectively alleviates layer-wise representation bias and bridges the performance gap between model merging based MTL and traditional MTL. Specifically, our *SurgeryV2* aligns the representation of the merged model with that of the individual models at *each layer*, thereby effectively mitigating MTL performance degradation.

We conduct numerous experiments to demonstrate the

SOTA performance of our *Surgery* and *SurgeryV2* schemes (§V). Our comprehensive evaluation covered eight vision datasets, five text datasets, four representative model merging methods, and four model architectures within the computer vision (CV) and natural language processing (NLP) domains. Our observations include the following: (i) when *Surgery* and *SurgeryV2* schemes are applied to existing model merging methods, the merged model achieves significantly better MTL performance. In particular, as shown in Fig. 1, our *SurgeryV2* model merging scheme achieves comparable or even slightly better performance than the traditional MTL method, which is noteworthy. (ii) By monitoring the performance changes during the optimization process, we find that with the same capacity, *SurgeryV2* can achieve significantly higher accuracy than *Surgery* with fewer iterations. (iii) Our proposed *SurgeryV2* is effective even in wild data settings, significantly broadening its range of application scenarios.

The **main contributions** of this paper are as follows:

- We revisit representative model merging methods and, for the first time, identify the “representation bias” problem (which exists across tasks, architectures, and merging methods) as a major cause of poor MTL performance.
- We propose a novel “representation surgery” approach, termed *Surgery*, to mitigate “representation bias” in the merged model. Notably, the *Surgery* module is suitable for any existing model merging algorithm.
- We reveal the correlation between the capacity of *Surgery* module and the degree to which representation bias is resolved. Furthermore, we find that representation bias occurs in each layer of the merged model, and addressing this bias solely in the final layer is insufficient.
- We introduce a deep representation surgery scheme (also called *SurgeryV2*), which applies representation surgery to each layer of the merged model, effectively reducing layer-wise representation bias.
- We conduct extensive experiments across CV and NLP domains, including eight vision datasets, five text datasets, four model architectures, and four representative model merging methods. The results substantiate the effectiveness of both our *Surgery* and *SurgeryV2*.

II. RELATED WORKS

In this section, we briefly introduce the related work, with a more comprehensive discussion provided in Appendix VII.

Recent studies have attempted to achieve MTL using model merging techniques [32, 22, 40, 41, 33]. However, the performance of simple parameter averaging [34, 42] degrades significantly as the number of tasks increases, resulting in a substantial gap between its performance and that of traditional MTL model. Many recent works have made various attempts to fill this gap [36, 21, 29, 24, 43, 25, 23, 44, 26, 33]. The *first type* of method explores how to better weigh and combine multiple models [19, 45, 40]. For example, Fisher-Merging [19] performs weighted merging utilizing the importance of each parameter through the Fisher information matrix [46]. RegMean [24] reweights and linearly combines rows in weight matrices based on statistics from training data. AdaMerging [26] leverages unlabeled test data to automatically learn a set of task-level or layer-level model merging coefficients. The *second type* of method explores how to merge models in sparse subspaces to reduce interference [47, 48, 30, 49, 50, 31, 51]. For example, Ties-Merging [21] removes the smaller magnitude parameters and eliminates the issue of parameter sign conflicts during model merging. DARE [29] removes a large number of useless neuron updates and then scales the neurons for merging. Concrete [52] finds a shared subspace between multiple tasks for model merging. The *third type* of method dynamically merges multiple expert modules during inference [53, 54, 55, 56, 57]. For example, WEMoE [53] dynamically merges linear layers by routing, and static merges nonlinear layers. It should be noted that the dynamic merging method requires additional maintenance of more model parameters than the first two categories of methods, and it also reduces the inference efficiency.

While existing methods predominantly concentrate on merging in weight space, they often neglect a crucial concern stemming from weight merging—the *representation bias*. A substantial disparity emerges in the *representation space* between the merged model and individually trained expert models. In contrast, our method addresses this gap, aiming to minimize the representation discrepancy. Moreover, our approach operates in the *representation space*, offering a complementary and orthogonal perspective to traditional weight-space merging methods. Consequently, our method can be seamlessly integrated with them.

III. PRELIMINARY

In this section, we first define the notation within the context of model merging (§III-A), and then introduce some representative model merging solutions (§III-B).

A. Notations and Problem Setting

Notations: Assume there are T models $(\Phi_{\Theta^{(1)}}, \dots, \Phi_{\Theta^{(T)}})$ of the same architecture that needs to be merged, and they are fine-tuned into a pretrained model $\Phi_{\Theta^{(0)}}$ on tasks $1 - T$ respectively. The parameters (or weights) of the t -th model $\Phi_{\Theta^{(t)}}$ are represented as $\Theta^{(t)} = \{\Theta_l^{(t)}\}_{l=1}^L$, where l denotes

the l -th layer¹ of the model, and L is the total number of layers. In addition, the test set of the t -th task is defined as $\mathcal{D}_{te}^{(t)} = \{\mathcal{X}^{(t)}, \mathcal{Y}^{(t)}\} = \{x_i^{(t)}, y_i^{(t)}\}_{i=1}^{|\mathcal{D}_{te}^{(t)}|}$, where $x_i^{(t)}$ represents the i -th input sample and $y_i^{(t)}$ represents the corresponding label, and $|\mathcal{D}_{te}^{(t)}|$ is the number of samples. Without loss of generality, the forward propagation of a deep neural network model can be represented as a directed acyclic computation graph, where the output of each layer serves as the input for the subsequent layer. Based on these notations, we give definitions of representations and model merging in Definition III.1 and Definition III.2, respectively.

Definition III.1 (Representation). Given a model $\Phi_{\Theta^{(t)}}$, we define the output (also referred to as *representation*) of sample $x_i^{(t)}$ at the l -th layer as $z_{l,i}^{(t)} = \Phi_{\Theta^{(t)}}(x_i^{(t)}) \in \mathbb{R}^{d_l}$, and d_l represents the output dimension of the l -th layer. Similarly, the representation of all samples for task t at the l -th layer is denoted by $\mathbf{Z}_l^{(t)} = \{z_{l,i}^{(t)}\}_{i=1}^{|\mathcal{D}_{te}^{(t)}|} \in \mathbb{R}^{d_l \times |\mathcal{D}_{te}^{(t)}|}$.

Definition III.2 (Model Merging). Given multiple expert models fine-tuned on different tasks, the goal of model merging is to merge the parameters $\{\Theta^{(1)}, \dots, \Theta^{(T)}\}$, and finally obtain the new parameters $\Theta^{(mtl)} = \text{merge}(\Theta^{(1)}, \dots, \Theta^{(T)})$, and $\Phi_{\Theta^{(mtl)}}$ can successfully perform tasks $1 - T$. In other words, the objective of model merging is for the MTL model $\Phi_{\Theta^{(mtl)}}$ to achieve the lowest loss on test sets of all tasks, which is defined as follows:

$$\arg \min_{\Theta^{(mtl)}} \frac{1}{T} \sum_{t=1}^T \sum_{i=1}^{|\mathcal{D}_{te}^{(t)}|} \frac{1}{|\mathcal{D}_{te}^{(t)}|} \mathcal{L}^{(t)} \left(\Phi_{\Theta^{(mtl)}}(x_i^{(t)}), y_i^{(t)} \right), \quad (1)$$

where $\Theta^{(mtl)} = \text{merge}(\Theta^{(1)}, \dots, \Theta^{(T)})$,

where $\mathcal{L}^{(t)}(\cdot)$ is the loss function for the t -th task, such as cross-entropy loss or mean squared error.

Taking two tasks as an example, as illustrated in Fig. 8, model merging hopes to combine the expert models trained individually on task A and task B (i.e., Fig. 8(a)) to obtain a new model (i.e., Fig. 8(b)) capable of performing both tasks A and B . Mainstream model merging research focuses on designing more advanced $\text{merge}(\cdot)$ strategies to alleviate task conflict and task interference [35, 36, 24, 21, 29, 26, 48].

B. Representative Model Merging Methods

In this section, based on the popularity and performance of model merging methods, we select four representative methods to introduce: Weighted Averaging [34], Task Arithmetic [36], Ties-Merging [21], and AdaMerging [26].

When merging models, one of the simplest solutions is **Weighted Averaging**, defined as $\Theta^{(mtl)} = \frac{1}{T} \sum_{t=1}^T \Theta^{(t)}$. However, it often results in suboptimal performance due to potential task conflicts. As mentioned in §II, a lot of advanced work has been devoted to developing better merge operations (i.e., the $\text{merge}(\cdot)$ function in Eq. 1) to reduce the performance degradation of the merged model $\Phi_{\Theta^{(mtl)}}$ compared

¹This paper uses the terms of layer, block and module interchangeably, and they all refer to same concept.

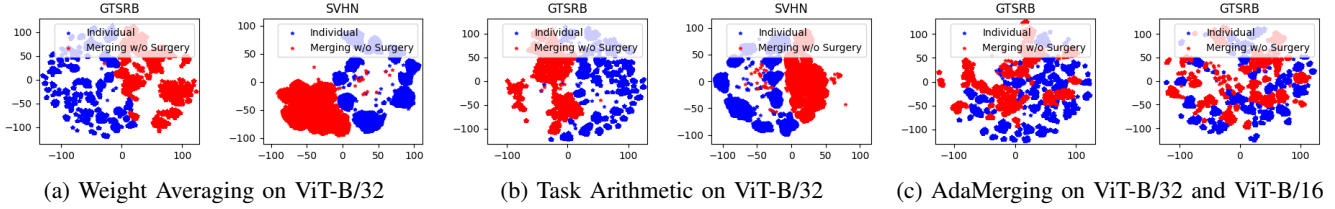


Fig. 2: Visualization of the distribution of representations extracted by the merged model (red) for the existing model merging schemes and representations extracted by the individual expert model (blue). We observe that there is a clear distribution discrepancy between the two.

to individual models $\{\Phi_{\Theta^{(1)}}, \dots, \Phi_{\Theta^{(T)}}\}$ or the traditional MTL model. As a representative work, *Task Arithmetic* [36] uses a grid search algorithm to find a better model merging coefficient λ , i.e., $\Theta^{(mtl)} = \Theta^{(0)} + \lambda \cdot \sum_{t=1}^T (\Theta^{(t)} - \Theta^{(0)})$, where $\Theta^{(0)}$ is the pre-trained model’s weight. Building on this approach, *Ties-Merging* [21] suggests that eliminating parameter sign conflicts prior to merging can reduce inter-model interference. Its merge rule is $\Theta^{(mtl)} = \Theta^{(0)} + \lambda \cdot \sum_{t=1}^T \phi(\Theta^{(t)} - \Theta^{(0)})$, where $\phi(\cdot)$ is a function that resolves sign conflicts. Subsequently, *AdaMerging* [26] emphasizes the critical impact of merging coefficients on performance. It proposes optimizing the layer-level merging coefficients $\lambda_l^{(t)}$ formalized as $\Theta^{(mtl)} = \{\Theta_l^{(0)} + \sum_{t=1}^T \lambda_l^{(t)} \cdot (\Theta_l^{(t)} - \Theta_l^{(0)})\}_{l=1}^L$.

These advanced works have achieved more powerful performance than the vanilla Weighted Averaging method. However, there is still a significant performance gap compared with individual models or the traditional MTL model. This motivates us to further analyze the reasons behind the limited performance of these model merging methods.

IV. METHOD

This section first re-examines these representative merging schemes from the perspective of representation distribution and establishes that they suffer from “representation bias” (§IV-A). Then, we propose a representation surgery (i.e., Surgery) method to mitigate representation bias (§IV-B). Despite the new SOTA performance achieved by Surgery, it still has gaps with traditional MTL or expert models. Next, we conduct an in-depth analysis of the Surgery scheme and reveal the phenomenon of layer-wise representation bias (§IV-C). Finally, we propose a deep representation surgery scheme (i.e., SurgeryV2) scheme to perform representation alignment at each layer of the merged model (§IV-D).

A. Revisiting Representation Bias

This section analyzes representative merging schemes mentioned in §III-B from the perspective of the representation distribution of the merged model and expert models and identifies a key issue that limits the MTL performance of the merged model, namely, “representation bias”. We give a clear definition of representation bias in Definition IV.1.

Definition IV.1 (Representation Bias). Given merged model $\Phi_{\Theta^{(mtl)}}$ and individual expert models $\{\Phi_{\Theta^{(1)}}, \dots, \Phi_{\Theta^{(T)}}\}$, the representation bias $b_L^{(t)}$ w.r.t. task t is defined as the discrepancy between the representations $\mathbf{Z}_L^{(t), ind}$ and $\mathbf{Z}_L^{(t), mtl}$

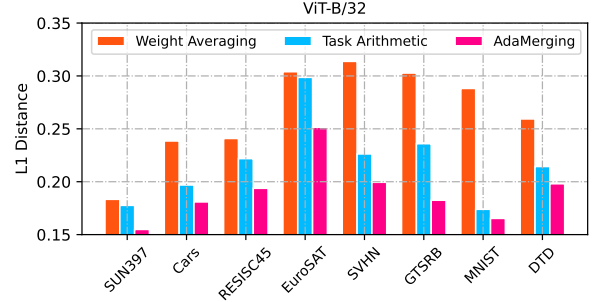


Fig. 3: The “representation bias” (in Eq. 2 of Definition IV.1) between representations extracted by the merged model using three model merging methods and representations extracted by individual expert models.

extracted from the *final* (i.e., L -th) layer of the individual expert model $\Phi_{\Theta^{(t)}}$ and the merged model $\Phi_{\Theta^{(mtl)}}$:

$$b_L^{(t)} = \frac{1}{|\mathcal{D}_{te}^{(t)}|} \frac{1}{d_L} \psi \left(\mathbf{Z}_L^{(t), mtl}, \mathbf{Z}_L^{(t), ind} \right), \quad (2)$$

where $\psi(\cdot)$ represents any distance-measuring function, such as L_1 or L_2 loss, and d_L is the dimension of the representation at the final layer (e.g., ViT-B/32 and ViT-B/16 are 512, and ViT-L/14 is 768).

Without loss of generality, we perform analysis on the following representative model merging methods, tasks/datasets, and architectures: (i) **Methods:** We analyze the four model merging methods mentioned in §III-B. (ii) **Tasks:** We follow Task Arithmetic [36] and use the following eight datasets as eight tasks for model merging: SUN397, Cars, RESISC45, EuroSAT, SVHN, GTSRB, MNIST, DTD. We provide a detailed dataset description in Appendix VIII. (iii) **Architectures:** We merge eight expert models into one model and experiment with three ViT architectures [39] with different parameter scales: ViT-B/32, ViT-B/16, and ViT-L/14.

To reveal the performance gap between the merged model $\Phi_{\Theta^{(mtl)}}$ and the individual expert models $\{\Phi_{\Theta^{(1)}}, \dots, \Phi_{\Theta^{(T)}}\}$, we use the t-SNE [58] tool to visualize the representations $\mathbf{Z}_L^{(t), ind}$ and $\mathbf{Z}_L^{(t), mtl}$ of the expert and merged models, as well as directly measure the representation bias in Definition IV.1. We find that “representation bias” exists **across tasks, across merging methods, and across architectures**:

- From the perspective of the representation distribution ². As shown in Fig. 2, we have the following observations: (i)

²Due to space limitations, we only show two tasks (GTSRB and SVHN), three merging methods (Weight Averaging, Task Arithmetic, and AdaMerging), and two architectures (ViT-B/32 and ViT-B/16) in the main text.

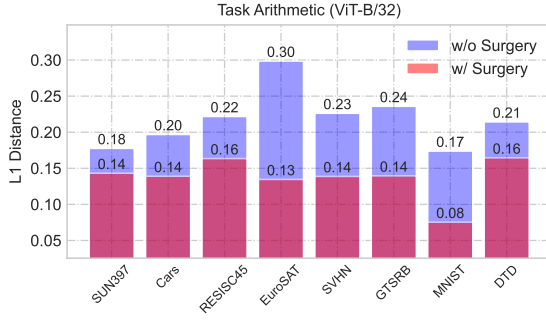


Fig. 4: Visualization of the “representation bias” (in Eq. 2) of the representation of the merged model **with** (red) and **without** (blue) representation surgery versus the individual model.

Across different tasks: As shown in Fig. 2(a), on the two tasks of GTSRB and SVHN, the representation distributions of the merged model (red points) and the individual expert model (blue points) are quite different. (ii) Across different merging methods: Comparing Fig. 2 (a), (b), (c), we find that the phenomenon of inconsistent representation distribution between the merged model and the individual model exists in Weight Averaging, Task Arithmetic and AdaMerging. (iii) Across different architectures: In Fig. 2(c), we observe that there is also an inconsistency in the representation distribution under ViT-B/32 and ViT-B/16 architectures.

- *From the perspective of the representation bias.* We quantify the representation bias between independent and merged models according to Definition IV.1. As shown in Fig. 3, we clearly observe that AdaMerging has a smaller representation bias between the merged model and the individual models compared to the other two model merging methods, i.e., Task Arithmetic and Weight Averaging. Meanwhile, Task Arithmetic also has a smaller representation bias than the Weight Averaging method.

This phenomenon inspires us to think: **Is representation bias the key factor limiting the MTL performance improvement of model merging?** We give a *positive* answer. On the one hand, previous research results [26, 21, 36] and the performance comparison in this paper (e.g., Tab. I, Tab. II and Tab. V (in Appendix IX-A)) show that in terms of the MTL performance of the merged model: AdaMerging > Task Arithmetic > Weight Averaging. On the other hand, our results in Fig. 2 and Fig. 3 show that AdaMerging < Task Arithmetic < Weight Averaging, whether in terms of representation distribution or representation bias. Therefore, MTL performance and representation bias show a strong positive correlation.

The above analysis demonstrates that “*representation bias*” *presents substantial challenges in model merging-based MTL.* The merged model’s performance improves as the representation bias decreases, motivating us to develop a solution to mitigate this issue in model merging-based MTL methods.

B. Surgery: Representation Surgery

In this section, to alleviate the representation bias, a novel representation surgery scheme is proposed, which involves aligning $\mathbf{Z}_L^{(t),ind}$ and $\mathbf{Z}_L^{(t),mtl}$ for task t using a representation

surgery module $\Omega_{\mathbf{W}^{(t)}}(\cdot)$ as Fig. 8(c). The formal objective function is defined as:

$$\min_{\{\mathbf{W}^{(1)}, \dots, \mathbf{W}^{(T)}\}} \sum_{t=1}^T \frac{1}{|\mathcal{D}_{te}^{(t)}|} \psi(\hat{\mathbf{Z}}_L^{(t),mtl}, \mathbf{Z}_L^{(t),ind}), \quad (3)$$

where $\hat{\mathbf{Z}}_L^{(t),mtl} = \mathbf{Z}_L^{(t),mtl} - \Omega_{\mathbf{W}^{(t)}}(\mathbf{Z}_L^{(t),mtl})$,

where $\psi(\cdot)$ is an arbitrary distance function, $\Omega_{\mathbf{W}^{(t)}}(\cdot)$ is an optimizable task-private lightweight module, which can be an arbitrary implementation (such as multiple fully connected layers, etc.). Without loss of generality, in this paper, we implement it as an Adapter-like structure [59], that is,

$$\Omega_{\mathbf{W}^{(t)}}(\mathbf{Z}_L^{(t),mtl}) = \mathbf{W}_{up}^{(t)} \cdot \text{ReLU}(\mathbf{W}_{down}^{(t)} \cdot (\mathbf{Z}_L^{(t),mtl})^\top), \quad (4)$$

where $\mathbf{W}_{up}^{(t)} \in \mathbb{R}^{d_L \times r}$, $\mathbf{W}_{down}^{(t)} \in \mathbb{R}^{r \times d_L}$ represent two learnable matrices, i.e., $\mathbf{W}^{(t)} = \{\mathbf{W}_{up}^{(t)}, \mathbf{W}_{down}^{(t)}\}$, $\text{ReLU}(\cdot)$ is a nonlinear activation function, d_L is the dimension of representation as mentioned in Definition III.1, and r is a hyperparameter, also called rank, which we set to 16 by default.

In particular, our Surgery scheme does not rely on any labeled training data. Instead, inspired by test-time adaptation [60, 61], it leverages the unlabeled test data $\{\mathcal{D}_{te}^t(\mathcal{X}, \mathcal{Y})\}_{t=1}^T$ and individual models $\{\Phi_{\Theta_t}\}_{t=1}^T$ as a self-supervised signal to optimize the parameters of the Surgery module, denoted as $\{\mathbf{W}^{(1)}, \mathbf{W}^{(t)}, \dots, \mathbf{W}^{(T)}\}$.

Discussion. The representation surgery proposed in this paper complements existing model merging schemes. We next discuss why the proposed Surgery scheme is effective. As mentioned in Eq. 4, the goal of the representation surgery is to reduce the discrepancy in the representation distributions between the merged and individual models. Comparing the discrepancy in representation distributions in Fig. 2 (w/o Surgery) and Fig. 5 (w/ Surgery), we can observe that the distributions of the merged and individual models in Fig. 5 are closer (i.e., higher overlap). In addition, we quantify the “representation bias” (in Definition IV.1) between the two distributions. As illustrated in Fig. 4, the proposed representation surgery (red column) significantly reduces the L_1 distance for the merged model compared to the model merged without representation surgery (blue column). For instance, on the EuroSAT dataset, Task Arithmetic-based model merging decreases the representation bias from 0.30 to 0.13 following representation surgery, representing a 56% relative reduction. These findings indicate that the proposed Surgery effectively mitigates the problem of representation bias.

C. Revisiting Representation Surgery

The representation surgery scheme mentioned in §III-B has indeed achieved significant performance improvements compared to existing model merging approaches. However, there is still a certain gap between it and the individual model or the traditional MTL model, irrespective of whether we consider representation distribution visualization or performance comparison. For example, in Fig. 5, the red and blue distributions exhibit imperfect overlap. Furthermore, as depicted in the left subfigure of Fig. 6, the optimal performance of Task Arithmetic with Surgery is 85.8, while the individual model is 90.5 and the traditional MTL model is 88.9. This encourages

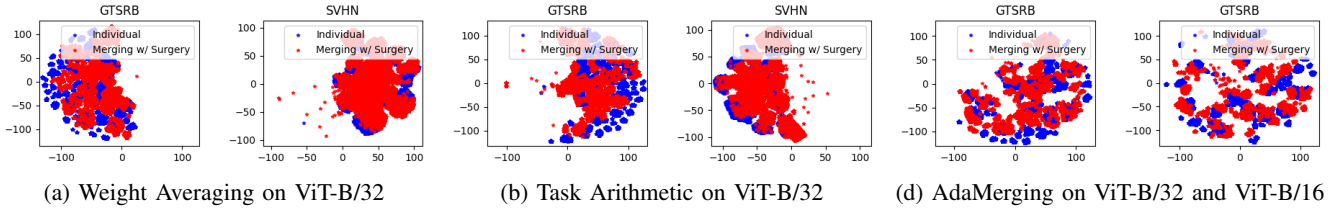


Fig. 5: Visualization of the distribution of features extracted by the merged model **after performing the representation surgery** (red) and features extracted by the individual model (blue). We observe that the two distributions overlap highly.

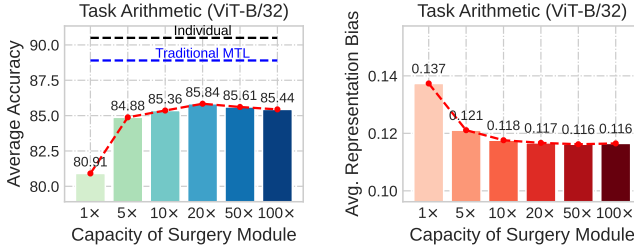


Fig. 6: An illustration of changes in the merged model’s performance (left, higher better) and representation bias (right, lower better) as the Surgery’s capacity increases.

us to intensify our efforts towards narrowing these gaps. In this section, by revisiting the Representation Surgery scheme (in §IV-B), we discerned two key observations.

Observation 1: *Increasing the surgery module’s capacity can enhance performance and reduce representation bias, but beyond a certain threshold, additional capacity has a negligible effect.* The Surgery module $\Omega_{\mathbf{W}^{(t)}}(\cdot)$ in Eq. 3 is a learnable module (e.g., a multi-layer perceptron or an Adapter-like module [59]), prompting a natural conjecture that expanding its capacity could ameliorate the representation bias and enhance performance. As depicted in Fig. 6, when we increase the capacity from $1\times$ to $20\times$, the average performance of the merged model increases from 80.9 to 85.8 (left subplot). Concomitantly, the representation bias at the last layer also decreased from 0.13 to 0.11 (right subplot). However, further increments in capacity, such as by a factor of $100\times$, do not yield substantial improvements in performance or bias. This suggests a ceiling (significantly lower than traditional MTL) on the efficacy of performing representation surgery at the *final layer* in alleviating representation bias.

Observation 2: *The “representation bias” problem exists at every layer of the merged model and increases monotonically with the layer’s depth.* Given that the forward propagation process of a deep neural network model follows a directed acyclic computation graph, the vanilla Surgery in §IV-B measures the representation bias and performs the representation surgery at the *last* layer. However, we argue that representation bias exists at every layer and interacts in complex ways. This leads to systemic bias in the final output that cannot be completely corrected by adjusting only the last layer. Specifically, as shown in Fig. 7³, by extending Definition IV.1, we quantify the representation bias $\{b_1^{(t)}, \dots, b_L^{(t)}\}$ of layer $\{1, \dots, L\}$

³Due to space limitations, Fig. 7 shows the average layer-wise representation bias across eight tasks. The layer-wise representation bias for each task is depicted in Fig. 13 and Fig. 14 in Appendix IX-D. Similar trends are observed across all eight tasks.

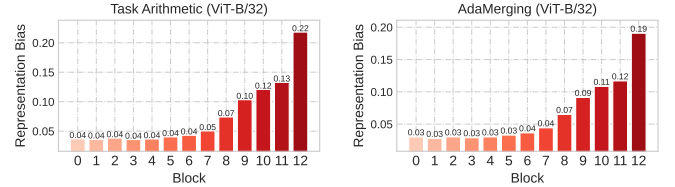


Fig. 7: An illustration of layer-wise representation bias. The x -axis represents the ID (or depth) of the block/layer, while the y -axis represents the representation bias of the corresponding layer. The four figures from left to right are combinations of two model merging methods (i.e., Task Arithmetic and AdaMerging) and ViT-B/32 architecture.

w.r.t task t following the definition provided in Definition IV.1. Observations reveal that: (i) The representation bias $b_l^{(t)}$ of every layer is non-zero and positive, indicating the presence of representation bias across all layers of the merged model. (ii) Representation bias monotonically increases with the layer’s depth, whereby deeper layers exhibit a larger bias compared to shallower ones. This phenomenon arises from the accumulation of representation bias from shallow to deep layers during forward propagation. These two observations remain consistent across various architectures, model merging methods, and datasets (eight datasets are shown in the Appendix IX-D), indicating their generality across different settings rather than being specific to particular instances.

Combining the observations mentioned above, we conclude that the **“representation bias” problem exists at every layer of the merged model**. Addressing “representation bias” only on the last layer as Surgery (§IV-B) is insufficient to fully resolve systemic representation bias, as biases introduced at each layer can accumulate and interact in complex ways.

D. SurgeryV2: Deep Representation Surgery

In this section, to more effectively address the issue of “representation bias” in the merged model, we introduce a novel deep representation surgery scheme, referred to as SurgeryV2 (as shown in Fig. 8(d)).

Unlike vanilla Surgery in §IV-B, which accumulates the representation biases from all layers to the *last* layer using a “lazy alignment” strategy, our SurgeryV2 scheme employs an “immediate alignment” strategy to perform representation surgery at *each* layer. Specifically, we first add a lightweight surgery module $\Omega_{\mathbf{W}^{(t)}}^l$ to each layer l w.r.t task t of the merged model $\Phi_{\Theta^{(mtl)}}$. Next, we align the representation $\hat{\mathbf{Z}}_l^{(t), mtl}$ of the merged model $\Phi_{\Theta^{(mtl)}}$ at layer $l \in \{1, \dots, L\}$ with the representation $\mathbf{Z}_l^{(t), ind}$ of the individual model $\Phi_{\Theta^{(t)}}$ at

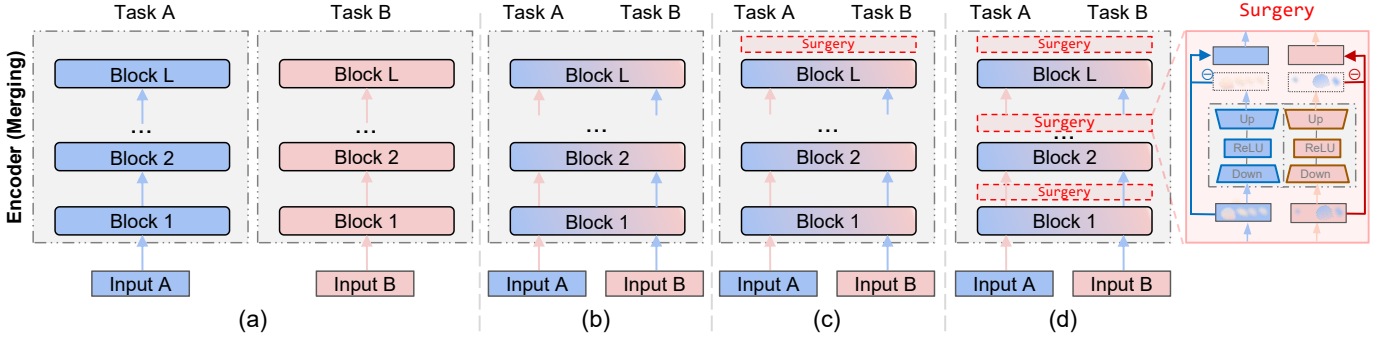


Fig. 8: An overview of model merging solutions: (a) individual models; (b) merged model produced by traditional model merging method (e.g., Weight Averaging, Task Arithmetic [36], Ties-Merging [21], AdaMerging [26]); (c) merged model employing our Surgery scheme in §IV-B; (d) merged model utilizing our SurgeryV2 scheme in §IV-D.

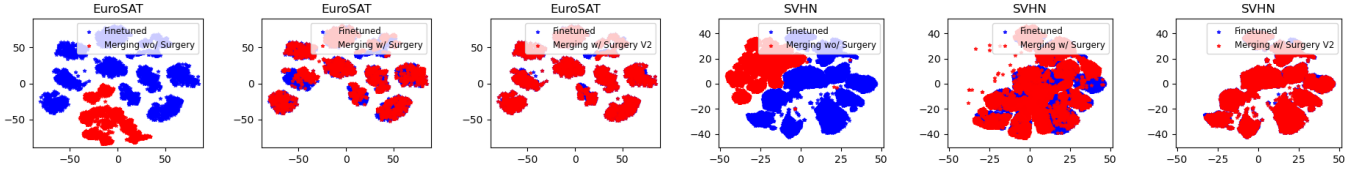


Fig. 9: Visualization of the distribution of final-layer representations for individual models (blue) and merged models (red) on EuroSAT and SVHN datasets. The *first column* represents the merged model obtained by Task Arithmetic without the representation surgery scheme. The *second column* indicates the use of the Surgery scheme from §IV-B, while the *third column* shows the results using our proposed SurgeryV2 scheme in §IV-D. Additional visualizations for more datasets are provided in Fig. 15, Fig. 16, Fig. 17, and Fig. 18 of Appendix IX-D.

the corresponding layer $l \in \{1, \dots, L\}$. Finally, the overall optimization goal of our SurgeryV2 method is defined as:

$$\min_{\{\mathbf{W}_1^{(1)}, \dots, \mathbf{W}_L^{(T)}\}} \sum_{t=1}^T \sum_{l=1}^L \frac{1}{|\hat{\mathcal{D}}|} \psi(\hat{\mathbf{Z}}_l^{(t), mtl}, \mathbf{Z}_l^{(t), ind}), \quad (5)$$

where $\hat{\mathbf{Z}}_l^{(t), mtl} = \mathbf{Z}_l^{(t), mtl} - \Omega_{\mathbf{W}_l^{(t)}}^l(\mathbf{Z}_l^{(t), mtl})$,

where T and L denote the number of tasks and layers, respectively. $\psi(\cdot)$ denotes an arbitrary distance function, which could be L_1 loss, mean squared error (MSE), or negative cosine similarity. Detailed comparisons of these different distance functions are provided in Tab. IX of Appendix IX-D. In addition, $\Omega_{\mathbf{W}_l^{(t)}}^l$ is a learnable lightweight module. Without loss of generality, we adopt an adapter-like [59] structure as described in §IV-B, which is,

$$\Omega_{\mathbf{W}_l^{(t)}}^l(\mathbf{Z}_l^{(t), mtl}) = \mathbf{W}_{l, \text{Up}}^{(t)} \text{ReLU}(\mathbf{W}_{l, \text{Down}}^{(t)} \cdot \mathbf{Z}_l^{(t), mtl}), \quad (6)$$

where $\mathbf{W}_l^{(t)} = \{\mathbf{W}_{l, \text{Up}}^{(t)}, \mathbf{W}_{l, \text{Down}}^{(t)}\}$, and $\mathbf{W}_{l, \text{Up}}^{(t)} \in \mathbb{R}^{d_l \times r}$ and $\mathbf{W}_{l, \text{Down}}^{(t)} \in \mathbb{R}^{r \times d_l}$ are two learnable weights within the SurgeryV2 module $\Omega_{\mathbf{W}_l^{(t)}}^l$, and r denotes a hyperparameter, which we set to 16 by default.

However, in the context of model merging, the labeled original training data is unavailable. To optimize $\{\mathbf{W}_l^{(t)}\}_{l=1, t=1}^{L, T}$ in SurgeryV2, drawing inspiration from test-time adaptation [60, 62], we leverage unlabeled test data. Furthermore, we also verified that the proposed SurgeryV2 can still work with wild data, although with a slight reduction in performance. Specifically, (i) In the case of SurgeryV2 with Unlabeled Test-time Data, we set $\hat{\mathcal{D}}$ in Eq. 5 to $\mathcal{D}_{te}^{(t)}$ as detailed in §III-A. (ii) In the case of SurgeryV2 with the

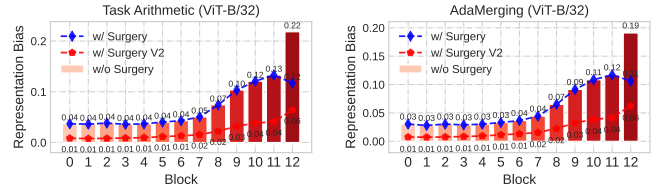


Fig. 10: Visualization of layer-wise representation bias (lower better). The left and right figures show the two model merging methods of Task Arithmetic and AdaMerging, respectively. In these figures, the red column indicates the representation bias of the merged model without the surgery scheme. The blue polyline and red polyline represent the representation bias after using the Surgery scheme from §IV-B and the SurgeryV2 scheme proposed in §IV-D, respectively. Note that these results are averaged over eight tasks, and the individual layer-wise representation biases for each task shown in Fig. 13 and Fig. 14 in the Appendix IX-D.

Wild Data, we utilize some easily accessible public data as $\hat{\mathcal{D}}$ in Eq. 5, e.g., benchmark data like ImageNet [63] in the CV domain, and data from Wikipedia in the NLP domain. The robust performance under wild data significantly broadens the applicability of our method.

Discussion. When the representation surgery is exclusively applied to the *last layer* as described in Eq. 5, our SurgeryV2 reverts to the vanilla Surgery approach in §IV-B. Indeed, our SurgeryV2 demonstrates notably enhanced effectiveness compared to that of Surgery in §IV-B, even when operating at equivalent capacity. Subsequently, we provide an analysis from two perspectives as follows:

• **Representation Bias.** As depicted in Fig 10, we evaluate

TABLE I: Multi-task performance when merging ViT-B/32 models on eight tasks. † indicates that Surgery uses the same number of parameters as SurgeryV2.

Method	SUN397	Cars	RESISC45	EuroSAT	SVHN	GTSRB	MNIST	DTD	Avg. †
Pretrained	62.3	59.7	60.7	45.5	31.4	32.6	48.5	43.8	48.0
Individual	75.3	77.7	96.1	99.7	97.5	98.7	99.7	79.4	90.5
Traditional MTL	73.9	74.4	93.9	98.2	95.8	98.9	99.5	77.9	88.9
Weight Averaging	65.3	63.4	71.4	71.7	64.2	52.8	87.5	50.1	65.8
Fisher Merging [19]	68.6	69.2	70.7	66.4	72.9	51.1	87.9	59.9	68.3
RegMean [24]	65.3	63.5	75.6	78.6	78.1	67.4	93.7	52.0	71.8
Task Arithmetic [36]	55.2	54.9	66.7	78.9	80.2	69.7	97.3	50.4	69.1
Ties-Merging [21]	65.0	64.4	74.8	77.4	81.2	69.3	96.5	54.5	72.9
AdaMerging [26]	64.5	68.1	79.2	93.8	87.0	91.9	97.5	59.1	80.1
Concrete AdaMerging [52]	67.8	70.0	87.5	96.0	91.6	96.7	98.7	63.8	84.0
Weight Averaging w/ Surgery (Ours)	67.6	64.6	85.8	96.8	76.9	82.9	97.8	67.3	80.0
Task Arithmetic w/ Surgery (Ours)	63.8	59.9	83.3	97.9	87.0	87.0	98.6	69.4	80.9
Ties-Merging w/ Surgery (Ours)	69.8	66.1	87.3	97.5	86.7	87.6	98.5	71.6	83.1
AdaMerging w/ Surgery (Ours)	69.8	71.0	88.9	98.1	91.7	96.5	98.8	73.6	86.1
Weight Averaging w/ Surgery† (Ours)	70.5	68.2	91.9	97.8	78.8	97.0	98.5	77.6	85.0
Task Arithmetic w/ Surgery† (Ours)	66.2	64.8	91.9	98.6	89.0	97.4	98.9	78.0	85.6
Ties-Merging w/ Surgery† (Ours)	71.5	69.7	92.6	98.5	88.6	97.3	99.0	78.7	87.0
AdaMerging w/ Surgery† (Ours)	71.6	72.3	93.6	99.0	92.7	98.4	99.1	78.7	88.2
Weight Averaging w/ SurgeryV2 (Ours)	72.1	67.6	94.1	99.4	96.0	98.2	99.4	77.0	88.0
Task Arithmetic w/ SurgeryV2 (Ours)	73.8	67.9	94.5	99.6	96.8	98.8	99.5	78.0	88.6
Ties-Merging w/ SurgeryV2 (Ours)	74.1	67.2	93.7	99.6	96.1	98.5	99.4	78.6	88.4
AdaMerging w/ SurgeryV2 (Ours)	74.7	71.4	95.1	99.6	96.8	98.9	99.6	78.3	89.3

the block-wise representation bias and observe that the merged model without any surgery scheme has a very large representation bias, while the Surgery scheme in §IV-B corrects the bias only in the last layer. For instance, in the case of the merged model generated through the Task Arithmetic method (left subfigure), the original Surgery reduces the bias of the last layer from 0.22 to 0.12. However, our SurgeryV2 not only further reduces the bias of the last layer to 0.06, but also effectively corrects bias from previous layers, for example, the biases of the first 6 layers approximate 0.01.

- **Representation Distribution.** We examined the level of overlap between the representation distributions extracted by the merged model and those by the individual model using the t-SNE [58] tool. Fig. 9 illustrates that the overlap between the distributions of SurgeryV2 (third column) is greater than that of the original Surgery (second column), whereas the overlap between the distributions without employing any surgery scheme (first column) is the lowest.

The aforementioned evidence indicates that SurgeryV2 holds greater promise in aligning the merged model with the individual expert models, thereby potentially achieving performance levels closer to those of the individual model (or traditional MTL model).

V. EXPERIMENT

This section presents the main results. Due to page limitations, additional experimental results and analysis are placed in the Appendix IX-A and Appendix IX-D, respectively.

A. Experimental Setup

The datasets, architectures, and baselines used in this paper are listed as follows. Further details can be found in Appendix VIII-B.

Datasets: Our experiments cover eight vision datasets and five text datasets. Following the setup of Task Arithmetic [36]

and AdaMerging [26], we treat the following eight datasets as eight tasks to perform model merging in the *CV domain*: SUN397 [37], Cars [38], RESISC45 [64], EuroSAT [65], SVHN [66], GTSRB [67], MNIST [68], DTD [69]. In addition, we treat the following five datasets from [70, 71] as five tasks to perform model merging in the *NLP domain*: AGNews (news classification), Yelp (sentiment analysis), Amazon (sentiment analysis), DBPedia (Wikipedia article classification) and Yahoo (questions and answers categorization).

Architectures: For vision data, we use three architectures: ViT-B/32, ViT-B/16, and ViT-L/14 from CLIP [72]. For text data, we use the commonly used BERT [73] model.

Baselines: We compared three *non-model merging* methods: Pretrained, Individual, and Traditional MTL models; seven popular *model merging* methods: Weight Averaging, Fisher Merging [19], RegMean [24], Task Arithmetic [36], Ties-Merging [21], AdaMerging [26], Concrete AdaMerging [52].

B. Performance Comparison

Computer Vision Domain. As shown in Tabs. I and II, we merged the models of ViT-B/32 and ViT-L/14 architectures well-trained on eight tasks, respectively. The observations are as follows: (i) The Individual model performs the best but requires separate model parameters for each task. Traditional MTL collaboratively trains a model on the original training data, and the performance is second-best. Pretrained model performs worst due to the lack of task-specific knowledge. (ii) Advanced model merging methods, such as Fisher Merging, RegMean, Task Arithmetic, Ties-Merging, AdaMerging and Concrete AdaMerging, outperform simple weight averaging. However, due to representation bias, a significant performance gap remains between these methods and the Traditional MTL paradigm. (iii) When our Surgery scheme is used in the existing model merging scheme, the performance of the merged model is significantly improved. However, since the representations are aligned only in the last layer, this scheme still

TABLE II: Multi-task performance when merging ViT-L/14 models on eight tasks. † indicates that Surgery uses the same number of parameters as SurgeryV2.

Method	SUN397	Cars	RESISC45	EuroSAT	SVHN	GTSRB	MNIST	DTD	Avg. †
Pretrained	66.8	77.7	71.0	59.9	58.4	50.5	76.3	55.3	64.5
Individual	82.3	92.4	97.4	100	98.1	99.2	99.7	84.1	94.2
Traditional MTL	80.8	90.6	96.3	96.3	97.6	99.1	99.6	84.4	93.5
Weight Averaging	72.1	81.6	82.6	91.9	78.2	70.7	97.1	62.8	79.6
Fisher Merging [19]	69.2	88.6	87.5	93.5	80.6	74.8	93.3	70.0	82.2
RegMean [24]	73.3	81.8	86.1	97.0	88.0	84.2	98.5	60.8	83.7
Task Arithmetic [36]	73.9	82.1	86.6	94.1	87.9	86.7	98.9	65.6	84.5
Ties-Merging [21]	76.5	85.0	89.3	95.7	90.3	83.3	99.0	68.8	86.0
AdaMerging [26]	79.0	90.3	90.8	96.2	93.4	98.0	99.0	79.9	90.8
Concrete AdaMerging [52]	77.8	91.2	92.1	97.0	94.4	97.9	99.0	79.5	91.1
Weight Averaging w/ Surgery (Ours)	73.7	83.9	92.0	98.4	82.4	86.3	98.7	71.9	85.9
Task Arithmetic w/ Surgery (Ours)	75.7	84.4	93.1	98.8	91.3	93.4	99.1	76.1	89.0
Ties-Merging w/ Surgery (Ours)	76.5	85.9	93.7	99.2	89.7	92.0	99.1	78.1	89.3
AdaMerging w/ Surgery (Ours)	80.3	90.8	94.3	98.2	94.1	98.7	99.2	82.5	92.3
Weight Averaging w/ Surgery† (Ours)	75.6	84.7	95.6	99.1	86.3	97.3	99.2	81.4	89.9
Task Arithmetic w/ Surgery† (Ours)	76.7	85.4	95.7	99.4	92.7	98.5	99.2	81.0	91.1
Ties-Merging w/ Surgery† (Ours)	77.4	87.2	95.7	99.5	91.3	98.2	99.3	81.9	91.3
AdaMerging w/ Surgery† (Ours)	80.4	91.1	95.5	99.2	94.9	99.0	99.3	83.2	92.8
Weight Averaging w/ SurgeryV2 (Ours)	77.5	86.2	96.0	99.5	97.8	99.1	99.6	81.3	92.1
Task Arithmetic w/ SurgeryV2 (Ours)	80.4	88.0	96.6	99.6	97.8	99.1	99.6	81.7	92.8
Ties-Merging w/ SurgeryV2 (Ours)	80.0	88.7	96.3	99.7	97.9	99.0	99.6	81.5	92.8
AdaMerging w/ SurgeryV2 (Ours)	83.8	91.5	96.7	99.6	97.9	99.1	99.6	84.0	94.0

TABLE III: Multi-task performance when merging BERT models on five tasks.

Method	AG News	Yelp Sentiment	Amazon Sentiment	Yahoo Q&A	DBPedia	Wikipedia	Avg. †
Individual	91.6	60.4	57.8	72.6	98.8		76.2
Traditional MTL	90.6	59.1	55.6	71.3	98.5		75.0
Weight Averaging	79.2	49.8	45.0	50.3	55.1		55.8
Task Arithmetic [36]	82.9	55.8	48.4	53.1	81.5		64.3
Weight Averaging w/ Surgery (Ours)	90.5	58.5	55.0	71.3	98.8		74.8
Task Arithmetic w/ Surgery (Ours)	89.9	58.0	55.8	71.0	98.4		74.6
Weight Averaging w/ SurgeryV2 (Ours)	90.5	60.3	57.4	72.0	98.8		75.8
Task Arithmetic w/ SurgeryV2 (Ours)	91.2	60.7	57.5	72.8	98.7		76.2

cannot reach the level of Traditional MTL most of the time. (iv) Our SurgeryV2 scheme enables the merged model’s performance to reach the Traditional MTL model’s level. For example, when AdaMerging is combined with SurgeryV2, the merged model (89.3 in ViT-B/32) even slightly exceeds the traditional MTL (88.9 in ViT-B/32).

Natural Language Processing Domain. We merged BERT models trained separately on five distinct text datasets. As shown in Tab. III, there is a clear performance gap between model merging based MTL (Weight Averaging and Task Arithmetic) and Traditional MTL. After performing our vanilla Surgery, the performance of Weight Averaging and Task Arithmetic improved from 55.8 and 64.3 to 74.8 and 74.6, respectively, yet it remains below that of Traditional MTL at 75.0. However, after performing our SurgeryV2, the performance of the merged model can be further improved to 75.8 and 76.2, which is very close to the performance of the individual model (i.e., 76.2). This demonstrates the effectiveness of our approach in the NLP domain.

C. Experimental Analysis

Surgery and SurgeryV2 with the Wild Data. In cases where unlabeled test data is insufficient for optimizing surgery modules (Eq. 3 in §IV-B and Eq. 5 in §IV-D), we investigated the possibility of utilizing public/auxiliary data as an alternative. For example, in the upper section of Tab. IV, we merge the models trained on the four datasets of AG, Yelp, Amazon,

and Yahoo, and use Wikipedia data for surgery. SurgeryV2 still achieves the same result as the Traditional MTL, which is 69.3, while the original Surgery only has 66.9. As shown in the lower section of Tab. IV, it is similar to using AG News as wild data to merge the corresponding models of Yelp, Amazon, Yahoo, and DBPedia. These results indicate that even with wild data, SurgeryV2 also demonstrates the wide applicability and potential to calibrate the merged model without requiring unlabeled test data.

Performance w.r.t. Iteration. As shown in Fig. 11, we show the performance changes during iterations of our Surgery and our SurgeryV2. For a fair comparison, the two maintain consistent representation capacity. We can observe that under the four model merging methods (Weight Averaging, Task Arithmetic, Ties-Merging, and AdaMerging), using our SurgeryV2 achieves higher final performance than the vanilla Surgery. Even the performance of SurgeryV2 in the 200-th iteration exceeds the performance of Surgery in 1000 iterations. This means our SurgeryV2 is more efficient.

VI. CONCLUSION AND FUTURE WORKS

In this paper, we first demonstrate that state-of-the-art model merging methods are affected by representation bias. To address this issue, we propose a representation surgery approach (i.e., Surgery) that aligns the merged model’s representations with those of the independent expert model at

TABLE IV: Multi-task performance when merging BERT models on four tasks in the wild data.

Method	Wild Data	AG News	Yelp Sentiment	Amazon Sentiment	Yahoo Q&A	Avg. \uparrow
Traditional MTL	-	90.0	59.5	56.9	70.8	69.3
Task Arithmetic [36]	-	81.4	57.3	51.4	45.8	59.0
Task Arithmetic w/ Surgery (Ours)	DBPedia Wikipedia	88.8	57.9	53.9	67.2	66.9
Task Arithmetic w/ SurgeryV2 (Ours)	DBPedia Wikipedia	90.6	60.1	55.5	71.1	69.3

Method	Wild Data	Yelp Sentiment	Amazon Sentiment	Yahoo Q&A	DBPedia Wikipedia	Avg. \uparrow
Traditional MTL	-	59.7	55.6	71.7	98.6	71.4
Task Arithmetic [36]	-	57.5	54.3	54.0	94.3	65.0
Task Arithmetic w/ Surgery (Ours)	AG News	55.0	55.5	66.4	97.6	68.6
Task Arithmetic w/ SurgeryV2 (Ours)	AG News	59.8	57.4	71.1	98.8	71.8

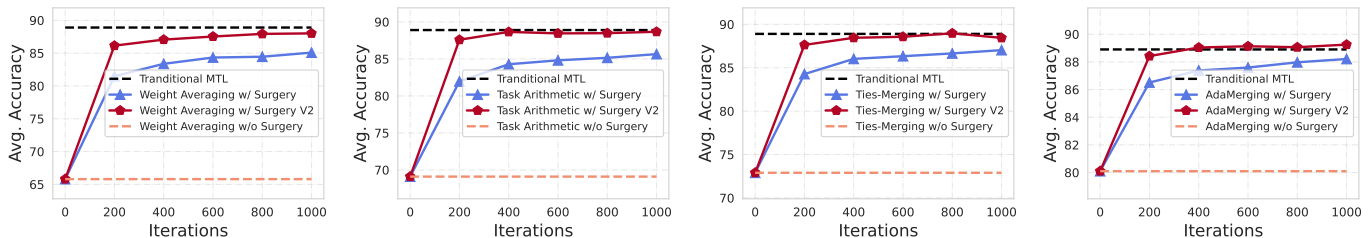


Fig. 11: An illustration of how the merged model’s performance varies with the number of iterations when merging eight ViT-B/32 models. From left to right, the plots represent model merging solutions based on Weight Averaging, Task Arithmetic, Ties-Merging, and AdaMerging.

the final layer, thereby mitigating the bias. However, the initial Surgery scheme still leaves a performance gap. Further analysis reveals that representation bias occurs across all layers of the merged model. To effectively alleviate this, we introduce a deep representation surgery scheme, termed SurgeryV2, which significantly reduces the representation bias. Experiments across CV and NLP tasks, merging methods, and architectures show that our solution matches traditional MTL performance. There are several directions for future research in our work: (i) developing a representation surgery strategy that eliminates the need for training, (ii) investigating model merging with different initializations or architectures; and (iii) extending the proposed representation surgery to a broader range of model merging scenarios.

REFERENCES

- [1] E. Yang, L. Shen, Z. Wang, G. Guo, X. Chen, X. Wang, and D. Tao, “Representation surgery for multi-task model merging,” *ICML*, 2024.
- [2] S. Vandenhende, S. Georgoulis, W. Van Gansbeke, M. Proesmans, D. Dai, and L. Van Gool, “Multi-task learning for dense prediction tasks: A survey,” *TPAMI*, vol. 44, no. 7, pp. 3614–3633, 2021.
- [3] S. Chen, Y. Zhang, and Q. Yang, “Multi-task learning in natural language processing: An overview,” *ACM Computing Surveys*, 2021.
- [4] S. J. Pan and Q. Yang, “A survey on transfer learning,” *TKDE*, vol. 22, no. 10, pp. 1345–1359, 2009.
- [5] G. Hadash, O. S. Shalom, and R. Osadchy, “Rank and rate: multi-task learning for recommender systems,” in *RecSys*, 2018, pp. 451–454.
- [6] Z. Chen, V. Badrinarayanan, C.-Y. Lee, and A. Rabinovich, “Gradnorm: Gradient normalization for adaptive loss balancing in deep multitask networks,” in *ICML*. PMLR, 2018, pp. 794–803.
- [7] Z. Chen, J. Ngiam, Y. Huang, T. Luong, H. Kretzschmar, Y. Chai, and D. Anguelov, “Just pick a sign: Optimizing deep multitask models with gradient sign dropout,” in *NeurIPS*, 2020.
- [8] B. Liu, X. Liu, X. Jin, P. Stone, and Q. Liu, “Conflict-averse gradient descent for multi-task learning,” *NeurIPS*, vol. 34, pp. 18 878–18 890, 2021.
- [9] E. Yang, J. Pan, X. Wang, H. Yu, L. Shen, X. Chen, L. Xiao, J. Jiang, and G. Guo, “Adatask: A task-aware adaptive learning rate approach to multi-task learning,” in *AAAI*, vol. 37, no. 9, 2023, pp. 10 745–10 753.
- [10] S. Liu, E. Johns, and A. J. Davison, “End-to-end multi-task learning with attention,” in *CVPR*. Computer Vision Foundation / IEEE, 2019, pp. 1871–1880.
- [11] O. Sener and V. Koltun, “Multi-task learning as multi-objective optimization,” in *NeurIPS*, 2018, pp. 525–536.
- [12] R. Collobert and J. Weston, “A unified architecture for natural language processing: Deep neural networks with multitask learning,” in *ICML*, 2008, pp. 160–167.
- [13] D. Dong, H. Wu, W. He, D. Yu, and H. Wang, “Multi-task learning for multiple language translation,” in *ACL*, 2015, pp. 1723–1732.
- [14] J. Ma, Z. Zhao, X. Yi, J. Chen, L. Hong, and E. H. Chi, “Modeling task relationships in multi-task learning with multi-gate mixture-of-experts,” in *SIGKDD*. ACM, 2018, pp. 1930–1939.
- [15] H. Tang, J. Liu, M. Zhao, and X. Gong, “Progressive layered extraction (ple): A novel multi-task learning (mtl) model for personalized recommendations,” in *RecSys*, 2020, pp. 269–278.
- [16] Y. He, X. Feng, C. Cheng, G. Ji, Y. Guo, and J. Caverlee, “Meta-balance: Improving multi-task recommendations via adapting gradient magnitudes of auxiliary tasks,” *WWW*, pp. 2205–2215, 2022.
- [17] M. Ravanelli, J. Zhong, S. Pascual, P. Swietojanski, J. Monteiro, J. Trmal, and Y. Bengio, “Multi-task self-supervised learning for robust speech recognition,” in *ICASSP*. IEEE, 2020, pp. 6989–6993.
- [18] X. Cai, J. Yuan, R. Zheng, L. Huang, and K. Church, “Speech emotion recognition with multi-task learning,” in *Interspeech*, vol. 2021. Brno, 2021, pp. 4508–4512.
- [19] M. S. Matena and C. A. Raffel, “Merging models with fisher-weighted averaging,” *NeurIPS*, vol. 35, pp. 17 703–17 716, 2022.
- [20] G. Ortiz-Jimenez, A. Favero, and P. Frossard, “Task arithmetic in the tangent space: Improved editing of pre-trained models,” *NeurIPS*, 2023.
- [21] P. Yadav, D. Tam, L. Choshen, C. Raffel, and M. Bansal, “Resolving interference when merging models,” *NeurIPS*, 2023.
- [22] G. Stoica, D. Bolya, J. Bjorner, T. Hearn, and J. Hoffman, “Zipit! merging models from different tasks without training,” *ICLR*, 2024.
- [23] J. Zhang, S. Chen, J. Liu, and J. He, “Composing parameter-

- efficient modules with arithmetic operations,” in *NeurIPS*, 2023.
- [24] X. Jin, X. Ren, D. Preotiuc-Pietro, and P. Cheng, “Dataless knowledge fusion by merging weights of language models,” in *ICLR*, 2023.
- [25] A. Ramé, G. Couairon, M. Shukor, C. Dancette, J.-B. Gaya, L. Soulier, and M. Cord, “Rewarded soups: towards pareto-optimal alignment by interpolating weights fine-tuned on diverse rewards,” in *NeurIPS*, 2023.
- [26] E. Yang, Z. Wang, L. Shen, S. Liu, G. Guo, X. Wang, and D. Tao, “Adamerging: Adaptive model merging for multi-task learning,” *ICLR*, 2024.
- [27] Z. Xu, K. Yuan, H. Wang, Y. Wang, M. Song, and J. Song, “Training-free pretrained model merging,” in *CVPR*, 2024.
- [28] A. Tang, L. Shen, Y. Luo, Y. Zhan, H. Hu, B. Du, Y. Chen, and D. Tao, “Parameter efficient multi-task model fusion with partial linearization,” *ICLR*, 2024.
- [29] L. Yu, B. Yu, H. Yu, F. Huang, and Y. Li, “Language models are super mario: Absorbing abilities from homologous models as a free lunch,” *ICML*, 2024.
- [30] K. Wang, N. Dimitriadis, G. Ortiz-Jimenez, F. Fleuret, and P. Frossard, “Localizing task information for improved model merging and compression,” *ICML*, 2024.
- [31] C. Huang, P. Ye, T. Chen, T. He, X. Yue, and W. Ouyang, “Emr-merging: Tuning-free high-performance model merging,” *NeurIPS*, 2024.
- [32] W. Li, Y. Peng, M. Zhang, L. Ding, H. Hu, and L. Shen, “Deep model fusion: A survey,” *arXiv preprint arXiv:2309.15698*, 2023.
- [33] E. Yang, L. Shen, G. Guo, X. Wang, X. Cao, J. Zhang, and D. Tao, “Model merging in llms, mllms, and beyond: Methods, theories, applications and opportunities,” *arXiv preprint arXiv:2408.07666*, 2024.
- [34] P. Izmailov, D. Podoprikin, T. Garipov, D. Vetrov, and A. G. Wilson, “Averaging weights leads to wider optima and better generalization,” *UAI*, 2018.
- [35] M. Wortsman, G. Ilharco, S. Y. Gadre, R. Roelofs, R. Gontijo-Lopes, A. S. Morcos, H. Namkoong, A. Farhadi, Y. Carmon, S. Kornblith *et al.*, “Model soups: averaging weights of multiple fine-tuned models improves accuracy without increasing inference time,” in *ICML*. PMLR, 2022, pp. 23 965–23 998.
- [36] G. Ilharco, M. T. Ribeiro, M. Wortsman, L. Schmidt, H. Hajishirzi, and A. Farhadi, “Editing models with task arithmetic,” in *ICLR*, 2023.
- [37] J. Xiao, K. A. Ehinger, J. Hays, A. Torralba, and A. Oliva, “Sun database: Exploring a large collection of scene categories,” *IJCV*, vol. 119, pp. 3–22, 2016.
- [38] J. Krause, M. Stark, J. Deng, and L. Fei-Fei, “3d object representations for fine-grained categorization,” in *ICCV workshops*, 2013, pp. 554–561.
- [39] A. Dosovitskiy, L. Beyer, A. Kolesnikov, D. Weissenborn, X. Zhai, T. Unterthiner, M. Dehghani, M. Minderer, G. Heigold, S. Gelly, J. Uszkoreit, and N. Houlsby, “An image is worth 16x16 words: Transformers for image recognition at scale,” *ICLR*, 2021.
- [40] T. Akiba, M. Shing, Y. Tang, Q. Sun, and D. Ha, “Evolutionary optimization of model merging recipes,” *arXiv preprint arXiv:2403.13187*, 2024.
- [41] N. Daheim, T. Möllenhoff, E. M. Ponti, I. Gurevych, and M. E. Khan, “Model merging by uncertainty-based gradient matching,” 2024.
- [42] B. McMahan, E. Moore, D. Ramage, S. Hampson, and B. A. y Arcas, “Communication-efficient learning of deep networks from decentralized data,” in *AISTATS*. PMLR, 2017, pp. 1273–1282.
- [43] C. Wu, T. Wang, Y. Ge, Z. Lu, R. Zhou, Y. Shan, and P. Luo, “pi-tuning: Transferring multimodal foundation models with optimal multi-task interpolation,” in *ICML*. PMLR, 2023, pp. 37 713–37 727.
- [44] N. Daheim, T. Möllenhoff, E. M. Ponti, I. Gurevych, and M. E. Khan, “Model merging by uncertainty-based gradient matching,” *ICLR*, 2024.
- [45] Y. Zhou, L. Song, B. Wang, and W. Chen, “Metagpt: Merging large language models using model exclusive task arithmetic,” *arXiv preprint arXiv:2406.11385*, 2024.
- [46] R. A. Fisher, “On the mathematical foundations of theoretical statistics,” *Philosophical transactions of the Royal Society of London. Series A, containing papers of a mathematical or physical character*, vol. 222, no. 594-604, pp. 309–368, 1922.
- [47] A. Panigrahi, N. Saunshi, H. Zhao, and S. Arora, “Task-specific skill localization in fine-tuned language models,” in *ICML*. PMLR, 2023, pp. 27 011–27 033.
- [48] G. Du, J. Lee, J. Li, R. Jiang, Y. Guo, S. Yu, H. Liu, S. K. Goh, H.-K. Tang, D. He *et al.*, “Parameter competition balancing for model merging,” *NeurIPS*, 2024.
- [49] M. Zimmer, C. Spiegel, and S. Pokutta, “Sparse model soups: A recipe for improved pruning via model averaging,” *ICLR*, 2024.
- [50] P. T. Deep, R. Bhardwaj, and S. Poria, “Della-merging: Reducing interference in model merging through magnitude-based sampling,” *arXiv preprint arXiv:2406.11617*, 2024.
- [51] M. Davari and E. Belilovsky, “Model breadcrumbs: Scaling multi-task model merging with sparse masks,” *arXiv preprint arXiv:2312.06795*, 2023.
- [52] A. Tang, L. Shen, Y. Luo, L. Ding, H. Hu, B. Du, and D. Tao, “Concrete subspace learning based interference elimination for multi-task model fusion,” *arXiv preprint arXiv:2312.06173*, 2023.
- [53] A. Tang, L. Shen, Y. Luo, N. Yin, L. Zhang, and D. Tao, “Merging multi-task models via weight-ensembling mixture of experts,” *ICML*, 2024.
- [54] M. Muqeeth, H. Liu, Y. Liu, and C. Raffel, “Learning to route among specialized experts for zero-shot generalization,” *ICML*, 2024.
- [55] P. Li, Z. Zhang, P. Yadav, Y.-L. Sung, Y. Cheng, M. Bansal, and T. Chen, “Merge, then compress: Demystify efficient smoe with hints from its routing policy,” *ICLR*, 2024.
- [56] Z. Lu, C. Fan, W. Wei, X. Qu, D. Chen, and Y. Cheng, “Twin-merging: Dynamic integration of modular expertise in model merging,” *arXiv preprint arXiv:2406.15479*, 2024.
- [57] P. Yadav, C. Raffel, M. Muqeeth, L. Caccia, H. Liu, T. Chen, M. Bansal, L. Choshen, and A. Sordoni, “A survey on model moerging: Recycling and routing among specialized experts for collaborative learning,” *arXiv preprint arXiv:2408.07057*, 2024.
- [58] L. Van der Maaten and G. Hinton, “Visualizing data using t-sne,” *Journal of machine learning research*, vol. 9, no. 11, 2008.
- [59] N. Houlsby, A. Giurgiu, S. Jastrzebski, B. Morrone, Q. De Laroussilhe, A. Gesmundo, M. Attariyan, and S. Gelly, “Parameter-efficient transfer learning for nlp,” in *ICML*. PMLR, 2019, pp. 2790–2799.
- [60] D. Wang, E. Shelhamer, S. Liu, B. Olshausen, and T. Darrell, “Tent: Fully test-time adaptation by entropy minimization,” in *ICLR*, 2021.
- [61] S. Niu, J. Wu, Y. Zhang, Z. Wen, Y. Chen, P. Zhao, and M. Tan, “Towards stable test-time adaptation in dynamic wild world,” in *ICLR*, 2023.
- [62] J. Liang, R. He, and T. Tan, “A comprehensive survey on test-time adaptation under distribution shifts,” *arXiv preprint arXiv:2303.15361*, 2023.
- [63] J. Deng, W. Dong, R. Socher, L.-J. Li, K. Li, and L. Fei-Fei, “Imagenet: A large-scale hierarchical image database,” in *CVPR*. Ieee, 2009, pp. 248–255.
- [64] G. Cheng, J. Han, and X. Lu, “Remote sensing image scene classification: Benchmark and state of the art,” *Proceedings of the IEEE*, vol. 105, no. 10, pp. 1865–1883, 2017.
- [65] P. Helber, B. Bischke, A. Dengel, and D. Borth, “Eurosat: A novel dataset and deep learning benchmark for land use and land cover classification,” *JSTARS*, vol. 12, no. 7, pp. 2217–2226, 2019.
- [66] N. Yuval, “Reading digits in natural images with unsupervised

- feature learning,” in *NIPS Workshop*, 2011.
- [67] J. Stallkamp, M. Schlipsing, J. Salmen, and C. Igel, “The german traffic sign recognition benchmark: a multi-class classification competition,” in *IJCNN*. IEEE, 2011, pp. 1453–1460.
- [68] Y. LeCun, “The mnist database of handwritten digits,” <http://yann.lecun.com/exdb/mnist/>, 1998.
- [69] M. Cimpoi, S. Maji, I. Kokkinos, S. Mohamed, and A. Vedaldi, “Describing textures in the wild,” in *CVPR*, 2014, pp. 3606–3613.
- [70] X. Zhang, J. Zhao, and Y. LeCun, “Character-level convolutional networks for text classification,” *NeurIPS*, vol. 28, 2015.
- [71] Y. Huang, Y. Zhang, J. Chen, X. Wang, and D. Yang, “Continual learning for text classification with information disentanglement based regularization,” in *NAACL*, 2021, pp. 2736–2746.
- [72] A. Radford, J. W. Kim, C. Hallacy, A. Ramesh, G. Goh, S. Agarwal, G. Sastry, A. Askell, P. Mishkin, J. Clark *et al.*, “Learning transferable visual models from natural language supervision,” in *ICML*. PMLR, 2021, pp. 8748–8763.
- [73] J. Devlin, M. Chang, K. Lee, and K. Toutanova, “BERT: pre-training of deep bidirectional transformers for language understanding,” in *NAACL*. Association for Computational Linguistics, 2019, pp. 4171–4186.
- [74] T. Y. Liu, A. Goh, and S. Soatto, “Tangent transformers for composition, privacy and removal,” *ICLR*, 2024.
- [75] A. Jacot, F. Gabriel, and C. Hongler, “Neural tangent kernel: Convergence and generalization in neural networks,” *NeurIPS*, vol. 31, 2018.
- [76] E. J. Hu, Y. Shen, P. Wallis, Z. Allen-Zhu, Y. Li, S. Wang, L. Wang, and W. Chen, “LoRA: Low-rank adaptation of large language models,” in *ICLR*, 2022.
- [77] S. P. Singh and M. Jaggi, “Model fusion via optimal transport,” *NeurIPS*, vol. 33, pp. 22 045–22 055, 2020.
- [78] S. Ainsworth, J. Hayase, and S. Srinivasa, “Git re-basin: Merging models modulo permutation symmetries,” in *ICLR*, 2023.
- [79] K. Jordan, H. Sedghi, O. Saukh, R. Entezari, and B. Neyshabur, “REPAIR: renormalizing permuted activations for interpolation repair,” in *ICLR*. OpenReview.net, 2023.
- [80] R. Caruana, “Multitask learning,” *Machine learning*, vol. 28, pp. 41–75, 1997.
- [81] W. Zhang, L. Deng, L. Zhang, and D. Wu, “A survey on negative transfer,” *IEEE/CAA Journal of Automatica Sinica*, vol. 10, no. 2, pp. 305–329, 2022.
- [82] X. Sun, R. Panda, R. Feris, and K. Saenko, “Adashare: Learning what to share for efficient deep multi-task learning,” *NeurIPS*, vol. 33, pp. 8728–8740, 2020.
- [83] I. Misra, A. Shrivastava, A. Gupta, and M. Hebert, “Cross-stitch networks for multi-task learning,” in *CVPR*. IEEE Computer Society, 2016, pp. 3994–4003.
- [84] Y. Gao, H. Bai, Z. Jie, J. Ma, K. Jia, and W. Liu, “Mtl-nas: Task-agnostic neural architecture search towards general-purpose multi-task learning,” in *CVPR*, 2020, pp. 11 543–11 552.
- [85] A. Kendall, Y. Gal, and R. Cipolla, “Multi-task learning using uncertainty to weigh losses for scene geometry and semantics,” in *CVPR*. IEEE Computer Society, 2018, pp. 7482–7491.
- [86] Y. Hu, R. Xian, Q. Wu, Q. Fan, L. Yin, and H. Zhao, “Revisiting scalarization in multi-task learning: A theoretical perspective,” in *NeurIPS*, 2023.
- [87] T. Yu, S. Kumar, A. Gupta, S. Levine, K. Hausman, and C. Finn, “Gradient surgery for multi-task learning,” *NeurIPS*, vol. 33, pp. 5824–5836, 2020.
- [88] Z. Wang and Y. Tsvetkov, “Gradient vaccine: Investigating and improving multi-task optimization in massively multilingual models,” in *ICLR*, 2021.
- [89] A. Navon, A. Shamsian, I. Achituve, H. Maron, K. Kawaguchi, G. Chechik, and E. Fetaya, “Multi-task learning as a bargaining game,” in *ICML*. PMLR, 2022, pp. 16 428–16 446.
- [90] L. Liu, Y. Li, Z. Kuang, J.-H. Xue, Y. Chen, W. Yang, Q. Liao, and W. Zhang, “Towards impartial multi-task learning,” in *ICLR*, 2021.
- [91] W.-H. Li and H. Bilen, “Knowledge distillation for multi-task learning,” in *ECCV 2020 Workshops*. Springer, 2020, pp. 163–176.
- [92] D. P. Kingma and J. Ba, “Adam: A method for stochastic optimization,” *arXiv preprint arXiv:1412.6980*, 2014.
- [93] A. Krizhevsky, G. Hinton *et al.*, “Learning multiple layers of features from tiny images,” 2009.

Appendix Overview. The content of this appendix is organized as follows:

VII Related Works	13
VII-A Model Merging for Multi-Task Learning . . .	13
VII-B Traditional Multi-Task Learning	13
VIII Experimental Details	14
VIII-A Datasets	14
VIII-B Baselines	14
VIII-C Implementation Details	15
IX Experimental Results and Analysis	15
IX-A Performance Comparison	15
IX-B SurgeryV2 in Online Setting	15
IX-C Surgery and SurgeryV2 in the Wild Data Setting	15
IX-D Component Analysis	16
IX-E Visualization	17

VII. RELATED WORKS

In this section, we discuss related work from two directions: model merging for multi-task learning in §VII-A and traditional multi-task learning in §VII-B.

A. Model Merging for Multi-Task Learning

Recent studies in the machine learning community have attempted to achieve MTL using model merging techniques [32, 22, 40, 41, 33]. However, the performance of simple parameter averaging [34, 42] degrades significantly as the number of tasks increases, resulting in a substantial gap between its performance and that of traditional MTL model. Many recent works have made various attempts to fill this gap. We divide model merging into two stages: before and during merging.

(i) The main concern **before merging** is how to provide more favorable preconditions for model merging, such as linearization or orthogonalization. Specifically, some works [20, 74] independently fine-tune each task in the Tangent space [75] of the pre-trained model and demonstrate that this helps disentangle the weight space from the input space, leading to better model merging. Similarly, Linearization-LoRA [28] linearly fine-tunes some LoRA modules [76] in Tangent space. In addition, Task Arithmetic [36] pointed out that the orthogonality between task vectors is one of the conditions for successful model merging. From the perspective of loss landscape, OTFusion [77], GitReBasin [78] and REPAIR [79] rearrange the neurons in each layer to facilitate weight interpolation.

(ii) The main focus **during merging** is how to mitigate interference and conflicts between models [36, 43, 21, 29, 24, 25, 23, 44, 26, 33]. The *first type* of method explores how to better weigh and combine multiple models [19, 45, 40]. For example, Fisher-Merging [19] performs weighted merging utilizing the importance of each parameter through the Fisher information matrix [46]. RegMean [24] reweights and linearly combines rows in weight matrices based on statistics from training data. AdaMerging [26] leverages unlabeled test data to automatically learn a set of task-level or layer-level model

merging coefficients. The *second type* of method explores how to merge models in sparse subspaces to reduce interference [47, 48, 30, 49, 50, 31, 51]. For example, Ties-Merging [21] removes the smaller magnitude parameters and eliminates the issue of parameter sign conflicts during model merging. DARE [29] removes a large number of useless neuron updates and then scales the neurons for merging. Concrete [52] finds a shared subspace between multiple tasks for model merging. PCB-Merging [48] utilizes intra-balancing to measure parameter importance in individual tasks and inter-balancing to assess parameter similarity between different tasks. The *third type* of method dynamically merges multiple expert modules during inference [53, 54, 55, 56, 57]. For example, WEMoE [53] dynamically merges linear layers by routing, and static merges nonlinear layers. It should be noted that the dynamic merging method requires additional maintenance of more model parameters than the first two categories of methods, and it also reduces the inference efficiency.

While existing methods predominantly concentrate on merging in weight space, they often neglect a crucial concern stemming from weight merging—the *representation bias*. A substantial disparity emerges in the *representation space* between the merged model and individually trained expert models. In contrast, our surgery method addresses this gap, aiming to minimize the representation discrepancy. Moreover, our approach operates in the *representation space*, offering a complementary and orthogonal perspective to traditional weight-space merging methods. Consequently, our method can be seamlessly integrated with them.

B. Traditional Multi-Task Learning

MTL uses one model to accommodate information from multiple tasks, which is very efficient in terms of computational efficiency [80, 2]. However, MTL usually faces negative transfer [80, 2, 81]. Existing work mainly solves the negative transfer problem from two directions: architecture and optimization. Specifically, (i) The classic SharedBottom [80] backbone performs poorly when tasks are not highly correlated. Advanced *architectures* primarily alleviate the phenomenon of negative transfer through modularization [14, 15], sparsification [82, 10], and soft sharing [83, 84] of the backbone. (ii) Other work alleviates task interference from an *optimization* perspective. For example, some works [85, 11, 10, 86] try to optimize the weight for each task loss. Some works [7, 87, 8, 88, 89] resolve multi-task gradient direction or sign conflicts. Other works [6, 90, 16, 9] try to eliminate the dominance of the learning rate or gradient. In particular, KD4MTL [91] uses the model trained on a single task as an additional supervised loss to guide the re-training of the MTL model, thereby alleviating the difficulty and magnitude imbalance of the loss in the MTL joint training.

Distinct from these existing traditional MTL approaches that concentrate on loss weight or gradient space to tackle the negative transfer issue, our method improves MTL performance by addressing the representation bias problem within the representation space in model merging based MTL, providing a novel and orthogonal perspective.

VIII. EXPERIMENTAL DETAILS

A. Datasets

Following Task Arithmetic [36], Ties-Merging [21] and AdaMerging [26], we merge the models trained on the following eight datasets.

- **SUN397** [37]: The database is a benchmark dataset for Scene Understanding (SUN) and contains a total of 108,753 images from 397 classes, where each class contains a different number of images, but each class has at least 100 images.
- **Cars** [38]: Stanford Cars is a dataset used for fine-grained recognition in the field of computer vision. It contains images of 196 car classes with a total of 16,185 images. The images of each class are divided roughly 1:1 into training set and test set.
- **RESISC45** [64]: The RESISC45 dataset is a publicly available benchmark for scene classification in remote sensing images. It contains 45 scene classes, and each class contains 700 images (each image resolution is 256×256), for a total of about 31,500 images.
- **EuroSAT** [65]: EuroSAT is a Sentinel-2-based satellite image dataset primarily used to classify land use in geospatial imagery and contains 27,000 labeled and georeferenced images in 10 classes.
- **SVHN** [66]: SVHN is a real image dataset containing 10 classes of color house number images, SVHN is very similar in style to MNIST [68] (handwritten digits in grayscale images), but it contains a larger number of images (more than 600,000 digital images).
- **GTSRB** [67]: The German Traffic Sign Recognition Benchmark (GTSRB) contains images with different lighting conditions and rich backgrounds. These images are classified into 43 classes of traffic signs, totaling more than 50,000 images.
- **MNIST** [68]: MNIST is a large database of handwritten digits in 10 classes that is one of the most famous datasets in machine learning. It contains 60,000 training images and 10,000 test images, each of which is 28×28 pixels.
- **DTD** [69]: The Describable Textures Dataset (DTD) contains 5,640 real labeled texture images, divided into 47 classes, each with about 120 images.

B. Baselines

The baselines we compare include three non-model merging methods, and seven representative model merging methods:

(i) Non-model Merging Methods:

- **Pretrained** directly uses the pre-trained model to test multiple downstream tasks. The performance of this method is generally less than acceptable due to the lack of task-related knowledge.
- **Individual** involves full fine-tuning of the pretrained model with task-specific training data and often yields superior performance. However, it requires maintaining a copy of model parameters for each task, which is very costly when the number of tasks is large.
- **Traditional MTL** collects data from multiple tasks and collaboratively trains a multi-task model. Due to potential

task interference, the performance of a multi-task model is usually slightly lower than that of individual models, but the advantage is that it only has a single model.

(ii) Model Merging Methods:

- **Weight Averaging** is the simplest model merging method, which directly adds the parameters of well-trained multiple models according to average values.
- **Fisher Merging** [19] measures the importance of each parameter based on the Fisher information matrix [46] and merges models based on that importance.
- **RegMean** [24] utilizes pre-computed inner product matrices of inputs at each layer from the original training data to conduct a linear combination of the model’s parameters.
- **Task Arithmetic** [36] defines the parameter difference between the fine-tuned model and the pre-trained model as a ‘task vector’, and merges multiple task vectors into the pre-trained model based on grid search coefficients for model merging.
- **Ties-Merging** [21] eliminates sign conflicts between parameters of task vectors based on Task Arithmetic [36], thereby effectively alleviating interference during model merging.
- **AdaMerging** [26] designed a layer-wise model merging strategy, which assigns a merging coefficient to each layer of the model to be merged and optimizes these coefficients by entropy minimization.
- **Concrete AdaMerging** [52] performs model merging in the shared subspace of multiple models. Similar to AdaMerging [26], it employs entropy minimization to identify the shared subspace.

(iii) Our Representation Surgery Methods: Our Surgery (in §IV-B) is orthogonal to the model merging methods in (ii). It points out that the merged model has ‘representation bias’ issue, and proposes to align the representation of the *last layer* of the individual model and the merged model to alleviate the bias. It contains the following four variants:

- **Weight Averaging w/ Surgery** performs representation surgery on the merged model by the Weight Averaging method.
- **Task Arithmetic w/ Surgery** carries out the representation surgery on the merged model via the Task Arithmetic [36] method.
- **Ties-Merging w/ Surgery** executes the surgery in the combined model through the Ties-Merging [21] method.
- **AdaMerging w/ Surgery** conducts the representation surgery within the model that has been merged using the AdaMerging [26] method.

(iv) Our Deep Representation Surgery Methods: Our SurgeryV2 (in §IV-D), like vanilla Surgery (in §IV-B), is also orthogonal to the model merging methods in (ii). In contrast to vanilla Surgery, we point out that ‘representation bias’ exists in every layer of the merged model, and therefore propose to perform representation surgery at *each layer* to align the representations of the individual model and the merged model. Furthermore, we incorporated the following four variants for experimental evaluation:

- **Weight Averaging w/ SurgeryV2** performs SurgeryV2 to correct the representation bias of the Weight Averaging merged model.

TABLE V: Multi-task performance when merging ViT-B/16 models on eight tasks. † indicates that Surgery uses the same number of parameters as SurgeryV2.

Method	SUN397	Cars	RESISC45	EuroSAT	SVHN	GTSRB	MNIST	DTD	Avg. ↑
Pretrained	63.8	64.6	65.7	54.5	52.0	43.3	51.7	45.1	55.0
Individual	81.8	86.8	96.9	99.7	97.8	99.1	99.7	82.0	92.9
Weight Averaging	67.7	70.0	75.3	79.5	74.9	60.1	94.4	43.8	70.7
Fisher-Merging [19]	68.5	69.9	75.2	80.4	73.2	61.2	94.5	50.7	71.7
RegMean [24]	69.1	71.6	77.6	88.8	83.7	70.2	96.9	54.6	76.6
Task Arithmetic [36]	61.1	65.9	74.0	76.2	88.0	73.9	98.4	53.0	73.8
Ties-Merging [21]	69.1	72.5	80.5	84.0	85.0	71.5	98.1	54.9	77.0
AdaMerging [26])	70.2	80.7	81.6	94.8	91.6	95.8	98.5	66.2	84.9
Weight Averaging w/ Surgery (Ours)	70.3	72.4	88.8	97.6	82.0	83.1	98.1	68.5	82.6
Task Arithmetic w/ Surgery (Ours)	68.3	72.3	88.7	97.7	91.0	89.5	98.9	72.9	84.9
Ties-Merging w/ Surgery (Ours)	73.0	76.2	90.7	98.1	89.7	86.7	98.7	75.2	86.0
AdaMerging w/ Surgery (Ours)	73.6	81.5	90.4	98.5	93.2	97.4	98.9	77.0	88.8
Weight Averaging w/ Surgery† (Ours)	73.6	78.3	93.9	98.6	84.5	96.8	99.0	81.2	88.2
Task Arithmetic w/ Surgery† (Ours)	71.2	76.8	93.6	99.0	92.1	97.8	99.2	80.4	88.8
Ties-Merging w/ Surgery† (Ours)	74.9	80.1	94.5	98.8	90.9	97.8	99.1	81.7	89.7
AdaMerging w/ Surgery† (Ours)	75.0	83.2	94.2	99.2	93.9	98.3	99.1	81.9	90.6
Weight Averaging w/ SurgeryV2 (Ours)	75.2	80.2	95.3	99.4	97.2	98.7	99.6	80.5	90.7
Task Arithmetic w/ SurgeryV2 (Ours)	77.5	80.8	95.7	99.5	97.4	98.8	99.5	80.3	91.2
Ties-Merging w/ SurgeryV2 (Ours)	77.7	81.3	96.0	99.6	97.4	99.0	99.5	80.0	91.3
AdaMerging w/ SurgeryV2 (Ours)	78.6	83.9	95.6	99.6	97.3	99.1	99.6	81.5	91.9

- **Task Arithmetic w/ SurgeryV2** conducts a SurgeryV2 on each layer of the merged model via Task Arithmetic [36] to align it with the individual model.
- **Ties-Merging w/ SurgeryV2** first obtains a merged model through Ties-Merging [21], and then executes the SurgeryV2 scheme proposed in this paper on it.
- **AdaMerging w/ SurgeryV2** performs SurgeryV2 on merged model by the AdaMerging [26].

C. Implementation Details

A critical hyperparameter in our Surgery or SurgeryV2 methods is the rank r in Eq. 4 (§IV-B) or Eq. 6 (§IV-D), which demonstrates the capacity of the representation surgery module. For the ViT-B/32 and ViT-B/16 architectures, we default it to 16; for the ViT-L/14 and BERT architectures, it defaults to 4. The results in Tab. X show that our method is very robust to the setting of rank (e.g., $r \in \{4, 6, 16, 32, 64\}$), and a smaller rank can also achieve satisfactory performance.

To optimize the parameters in the Surgery or SurgeryV2 module, we employ public data (e.g., ImageNet [63]) or unlabeled test data. We use the Adam optimizer [92] with a learning rate of 0.001 and a momentum of (0.9, 0.999) to update parameters. The batch size is set to 16, and the number of iterations is set to 1,000 by default. In addition, the loss function $\psi(\cdot)$ in Eq. 5 of SurgeryV2 (or Eq. 3 of Surgery) is set to the L_1 function by default.

We report the accuracy for each task, as well as the average accuracy (i.e., Avg.) across the eight vision tasks or five text tasks. Higher accuracy means better performance of the merged model.

IX. EXPERIMENTAL RESULTS AND ANALYSIS

In this section, we provide additional results and analyses that are omitted from the main text due to space constraints.

A. Performance Comparison

In Tab. I and Tab. II of the main text (§V-B), we show the performance of merging the ViT-B/32 and ViT-L/14 architectures. In Tab. V below, we further illustrate the results of merging ViT-B/16 models trained on eight vision tasks. The following significant and consistent phenomena can be observed: (i) Advanced model merging methods (e.g., Ties-Merging, AdaMerging) all achieve better performance than simple Weight Averaging. (ii) After using our Surgery to correct the representation bias problem of the merged model, the performance of the merged model has been significantly improved, especially under the optimal surgery capacity (results with †). (iii) Our SurgeryV2 achieves the highest performance by resolving the layer-wise representation bias.

B. SurgeryV2 in Online Setting

Under default settings, we rely on unlabeled test data to optimize parameters in SurgeryV2. In real-world scenarios, unlabeled test data may arrive in a streaming manner. Therefore, we evaluated the performance changes of SurgeryV2 in an online setting. Specifically, as shown in Tab. VI, we tested the performance of SurgeryV2 when $\{1\%, 10\%, 20\%, \dots, 100\%\}$ of test data is visible, with each sample being visible only once. We observe that the performance of the merged model increases significantly as the amount of available data grows. Even when only 1% of the data is visible once, using SurgeryV2 improves performance from 69.1 to 78.9, compared to the standard Task Arithmetic [36] method.

C. Surgery and SurgeryV2 in the Wild Data Setting

The standard Surgery in §IV-B and SurgeryV2 in §IV-D require parameter optimization (i.e., Eq. 3 and Eq. 5 in §IV). However, unlabeled test data may not always be available during model merging. Therefore, we verified the feasibility of executing Surgery and SurgeryV2 on public

TABLE VI: Impact of the amount of online test data on model performance in SurgeryV2 module.

Method	Available Test Set	SUN397	Cars	RESISC45	EuroSAT	SVHN	GTSRB	MNIST	DTD	Avg. \uparrow
Traditional MTL	-	73.9	74.4	93.9	98.2	95.8	98.9	99.5	77.9	88.9
Task Arithmetic [36]	-	55.2	54.9	66.7	78.9	80.2	69.7	97.3	50.4	69.1
Task Arithmetic w/ SurgeryV2 (Ours)	1%	68.8	61.7	76.6	84.0	94.6	88.2	98.5	51.9	78.0
Task Arithmetic w/ SurgeryV2 (Ours)	10%	72.5	64.2	89.2	95.8	96.8	96.9	99.3	59.8	84.3
Task Arithmetic w/ SurgeryV2 (Ours)	20%	73.9	66.5	92.3	98.2	97.0	97.9	99.5	64.4	86.2
Task Arithmetic w/ SurgeryV2 (Ours)	30%	74.5	68.4	92.7	98.4	97.0	98.4	99.6	66.8	86.9
Task Arithmetic w/ SurgeryV2 (Ours)	40%	74.8	70.5	93.6	99.2	97.1	98.5	99.6	68.8	87.7
Task Arithmetic w/ SurgeryV2 (Ours)	50%	75.3	70.3	94.3	99.3	97.0	98.4	99.5	69.7	87.9
Task Arithmetic w/ SurgeryV2 (Ours)	60%	75.3	70.0	94.1	99.3	97.1	98.6	99.6	71.8	88.2
Task Arithmetic w/ SurgeryV2 (Ours)	70%	75.7	71.1	94.4	99.6	97.3	98.5	99.6	72.4	88.5
Task Arithmetic w/ SurgeryV2 (Ours)	80%	75.7	70.7	94.5	99.3	97.0	98.6	99.6	74.5	88.7
Task Arithmetic w/ SurgeryV2 (Ours)	90%	75.7	71.8	94.6	99.5	97.2	98.7	99.6	74.3	88.9
Task Arithmetic w/ SurgeryV2 (Ours)	100%	76.0	70.9	94.5	99.6	97.2	98.9	99.5	75.1	88.9

TABLE VII: Multi-task performance when merging eight ViT-B/32 models under the wild data.

Method	Wild Data	SUN397	Cars	RESISC45	EuroSAT	SVHN	GTSRB	MNIST	DTD	Avg. \uparrow
Traditional MTL	-	73.9	74.4	93.9	98.2	95.8	98.9	99.5	77.9	88.9
Task Arithmetic [36]	-	55.2	54.9	66.7	78.9	80.2	69.7	97.3	50.4	69.1
Task Arithmetic w/ Surgery (Ours)	CIFAR100 [93]	52.1	52.7	67.0	62.5	82.1	63.6	95.6	45.2	65.1
Task Arithmetic w/ Surgery (Ours)	ImageNet [63]	62.6	56.5	70.8	74.2	79.4	63.5	96.1	58.2	70.2
Task Arithmetic w/ SurgeryV2 (Ours)	CIFAR100 [93]	65.4	50.2	77.7	87.5	95.0	93.5	98.9	53.1	77.7
Task Arithmetic w/ SurgeryV2 (Ours)	ImageNet [63]	72.2	63.6	87.3	97.8	93.5	91.3	98.1	69.5	84.2

TABLE VIII: Multi-task performance when performing Surgery at different blocks.

Method	Block ID	SUN397	Cars	RESISC45	EuroSAT	SVHN	GTSRB	MNIST	DTD	Avg. \uparrow
Traditional MTL	-	73.9	74.4	93.9	98.2	95.8	98.9	99.5	77.9	88.9
Task Arithmetic [36]	-	55.2	54.9	66.7	78.9	80.2	69.7	97.3	50.4	69.1
Task Arithmetic w/ Surgery (Ours)	Block #1	56.4	57.1	68.9	88.0	84.6	71.6	97.6	51.2	71.9
Task Arithmetic w/ Surgery (Ours)	Block #3	48.7	50.6	69.8	88.1	87.5	67.4	97.6	50.5	70.0
Task Arithmetic w/ Surgery (Ours)	Block #5	57.1	58.0	71.2	73.5	86.6	74.5	97.9	51.3	71.3
Task Arithmetic w/ Surgery (Ours)	Block #7	57.2	53.5	78.0	96.4	83.1	75.6	98.8	54.9	74.7
Task Arithmetic w/ Surgery (Ours)	Block #9	58.0	44.6	77.8	94.0	82.8	60.2	99.0	57.3	71.7
Task Arithmetic w/ Surgery (Ours)	Block #11	57.7	54.2	76.6	92.9	81.8	70.4	98.0	58.7	73.8
Task Arithmetic w/ Surgery (Ours)	Final Representation	64.2	58.4	83.1	97.8	86.7	87.6	98.7	69.3	80.7
Task Arithmetic w/ SurgeryV2 (Ours)	All Blocks	73.8	67.9	94.5	99.6	96.8	98.8	99.5	78.0	88.6

datasets. As shown in Tab. VII, without loss of generality, we use two commonly used benchmark datasets in the vision domain, CIFAR100 [93] and ImageNet [63], as auxiliary data to perform the representation surgery (e.g., our Surgery or our SurgeryV2).

The results show that, compared to Tab. I (in §V-B) when using unlabeled test data, the performance of the Surgery or SurgeryV2 using unlabeled test data has decreased under wild data conditions. However, compared to traditional Task Arithmetic [36], which does not employ representation surgery and achieves only an average accuracy of 69.1%, the proposed SurgeryV2 attains an accuracy of 84.2% on the ImageNet dataset. Under the CIFAR100 dataset, the performance will be lower, which may be due to the lower sample diversity and image resolution of CIFAR100 compared to ImageNet. Overall, our SurgeryV2 also achieved acceptable performance under wild data, greatly expanding the available scenarios of our SurgeryV2 solution.

D. Component Analysis

Surgery in Different Blocks. The analysis in §IV-C shows that the ‘representation bias’ phenomenon exists at each block of the merged model, prompting the question: What is the performance when conducting representation surgery on individual blocks? For instance, ViT-B/32 has a total of 12 blocks, and we tested the performance of performing Surgery operations on the {1, 3, 5, 7, 9, 11}-th block, the

final layer (i.e., the vanilla Surgery scheme in §IV-B), and all blocks (i.e., the SurgeryV2 scheme proposed in §IV-D).

As shown in Tab. VIII, the general trend is that the benefits are more obvious when the Surgery is performed on the posterior block. For example, the average accuracy of performing Surgery on the 1st block is 71.9, while the accuracy of performing Surgery on the 11-th block is 73.8, and the accuracy of performing Surgery on the last block is 80.7. Furthermore, our SurgeryV2 operates on all blocks, approaching performance (i.e., 88.6) closer to that of traditional MTL (i.e., 88.9).

Surgery and SurgeryV2 with Different Loss function.

The objective of the Surgery module and the SurgeryV2 module is to minimize the gap between the representation of the merged model and the representation of the individual expert model (Eq. 3 in §IV-B and Eq. 5 in §IV-D), thus making any distance-measuring function applicable. As shown in Tab. IX below, we tested the performance of using L_1 loss, mean-square error (MSE), and negative cosine similarity (Neg. Cos.) as loss functions. We can observe that under different loss functions, our scheme is significantly better than Task Arithmetic, which does not apply the surgery scheme. In particular, our SurgeryV2 achieves performance close to that of traditional MTL, indicating that our scheme is robust to different loss functions.

Surgery and SurgeryV2 with Different Ranks. One hyperparameter in Surgery and SurgeryV2 is rank (i.e., r of Eq. 4 in §IV-B or Eq. 6 in §IV-D), which reflects the

TABLE IX: Multi-task performance on the ViT-B/32 model with different loss functions.

Method	Loss Function	SUN397	Cars	RESISC45	EuroSAT	SVHN	GTSRB	MNIST	DTD	Avg. \uparrow
Traditional MTL	-	73.9	74.4	93.9	98.2	95.8	98.9	99.5	77.9	88.9
Task Arithmetic [36]	-	55.2	54.9	66.7	78.9	80.2	69.7	97.3	50.4	69.1
Task Arithmetic w/ Surgery (Ours)	L1 Loss	63.8	59.9	83.3	97.9	87.0	87.0	98.6	69.4	80.9
Task Arithmetic w/ Surgery (Ours)	MSELoss	64.3	59.8	84.0	97.8	87.6	88.7	98.8	69.8	81.4
Task Arithmetic w/ Surgery (Ours)	Neg. Cos.	63.8	59.2	84.5	97.5	88.8	86.4	99.0	70.3	81.2
Task Arithmetic w/ SurgeryV2 (Ours)	L1 Loss	73.8	67.9	94.5	99.6	96.8	98.8	99.5	78.0	88.6
Task Arithmetic w/ SurgeryV2 (Ours)	MSE Loss	74.0	70.2	94.7	99.4	95.9	98.3	99.4	77.6	88.7
Task Arithmetic w/ SurgeryV2 (Ours)	Neg. Cos.	74.3	70.6	94.7	99.8	96.3	98.6	99.6	77.8	88.9

TABLE X: Impact of the amount of rank on model performance in Surgery and SurgeryV2 modules.

Method	Rank (r)	SUN397	Cars	RESISC45	EuroSAT	SVHN	GTSRB	MNIST	DTD	Avg. \uparrow
Traditional MTL	-	73.9	74.4	93.9	98.2	95.8	98.9	99.5	77.9	88.9
Task Arithmetic [36]	-	55.2	54.9	66.7	78.9	80.2	69.7	97.3	50.4	69.1
Task Arithmetic w/ Surgery (Ours)	4	62.6	55.9	76.7	78.7	83.4	79.6	97.7	60.0	74.3
Task Arithmetic w/ Surgery (Ours)	8	63.2	58.5	79.9	93.9	84.5	82.1	98.5	64.2	78.1
Task Arithmetic w/ Surgery (Ours)	16	63.8	59.9	83.3	97.9	87.0	87.0	98.6	69.4	80.9
Task Arithmetic w/ Surgery (Ours)	32	64.7	62.4	87.3	98.3	88.3	92.8	98.8	72.5	83.1
Task Arithmetic w/ Surgery (Ours)	64	65.6	62.7	89.8	98.3	88.7	95.6	98.9	74.7	84.3
Task Arithmetic w/ SurgeryV2 (Ours)	4	72.7	68.1	93.8	99.5	96.4	98.1	99.6	76.3	88.1
Task Arithmetic w/ SurgeryV2 (Ours)	8	73.6	67.6	93.7	99.7	96.6	98.4	99.5	78.2	88.4
Task Arithmetic w/ SurgeryV2 (Ours)	16	73.8	67.9	94.5	99.6	96.8	98.8	99.5	78.0	88.6
Task Arithmetic w/ SurgeryV2 (Ours)	32	74.5	67.4	94.6	99.6	96.4	98.8	99.5	77.7	88.6
Task Arithmetic w/ SurgeryV2 (Ours)	64	74.3	72.1	94.4	99.7	96.9	98.2	99.4	77.6	89.1

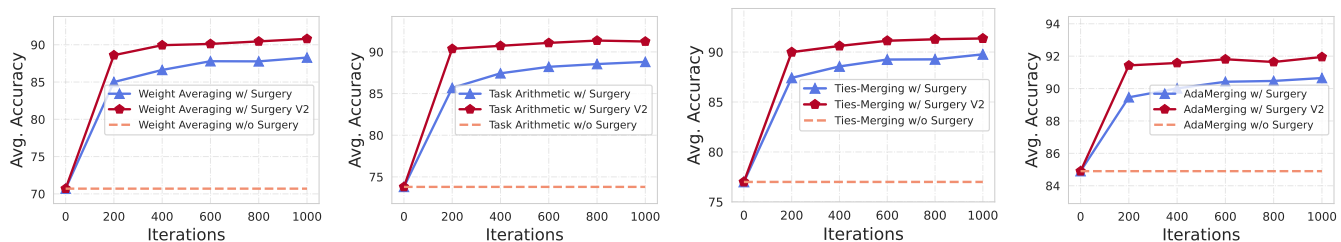


Fig. 12: An illustration of how the performance of the merged model changes w.r.t the number of iterations when merging eight ViT-B/16 models. From left to right are model merging solutions based on Weight Averaging, Task Arithmetic, Ties-Merging, and AdaMerging.

capacity of the Surgery module. As shown in Tab. X below, we evaluated the performance changes for various values of the rank r (e.g., $r \in \{4, 6, 8, 16, 32, 64\}$). We observe that the performance of the merged model improves as the rank increases. In particular, SurgeryV2 is very close to the performance of the traditional MTL model at different ranks.

Performance w.r.t. Iterations. Illustrated in Fig. 12, we show how the accuracy of our Surgery and our SurgeryV2 changes during iterations when merging eight ViT-B/16 models. It is evident that the SurgeryV2 method attains superior performance with fewer iterations compared to the vanilla Surgery method, ultimately yielding better final performance.

E. Visualization

Representation Bias. In Fig. 13 and Fig. 14, we show the block-wise representation bias on eight datasets, comparing two model merging techniques (i.e., Task Arithmetic [36] and AdaMerging [26]) under three conditions: without any surgery, with the original Surgery as proposed in §IV-B, and with our SurgeryV2 in §IV-D.

Representation Distribution. As shown in Fig. 15 and Fig. 16, we visualize the representation distributions of the original Task Arithmetic [36], the merged model that executes our Surgery or our SurgeryV2 on eight datasets.

Likewise, Fig. 17 and Fig. 18 represent visualizations of the AdaMerging [26] method.

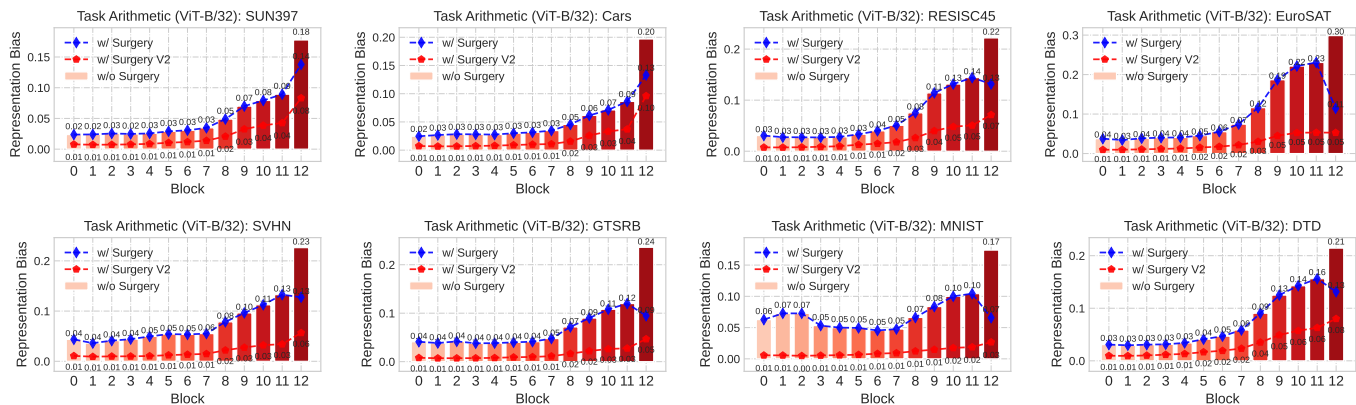


Fig. 13: Visualization of the distribution of extracted representations (final layer) for individual models (blue) and merged models (red) on eight datasets. The *first column* represents the merged model obtained by **Task Arithmetic** [36] (ViT-B/32) without using the representation surgery scheme. The *second column* indicates the use of the Surgery scheme in §IV-B, and the *third column* indicates the use of the SurgeryV2 scheme proposed in §IV-D.

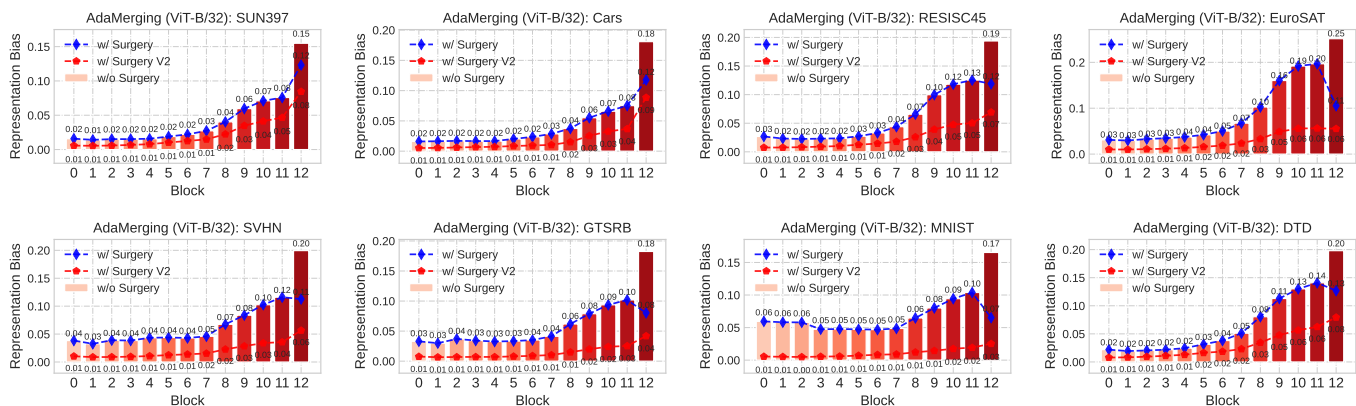


Fig. 14: Visualization of the distribution of extracted representations (final layer) for individual models (blue) and merged models (red) on eight datasets. The *first column* represents the merged model obtained by **AdaMerging** [26] (ViT-B/32) without using the representation surgery scheme. The *second column* indicates the use of the Surgery scheme in §IV-B, and the *third column* indicates the use of the SurgeryV2 scheme proposed in §IV-D.

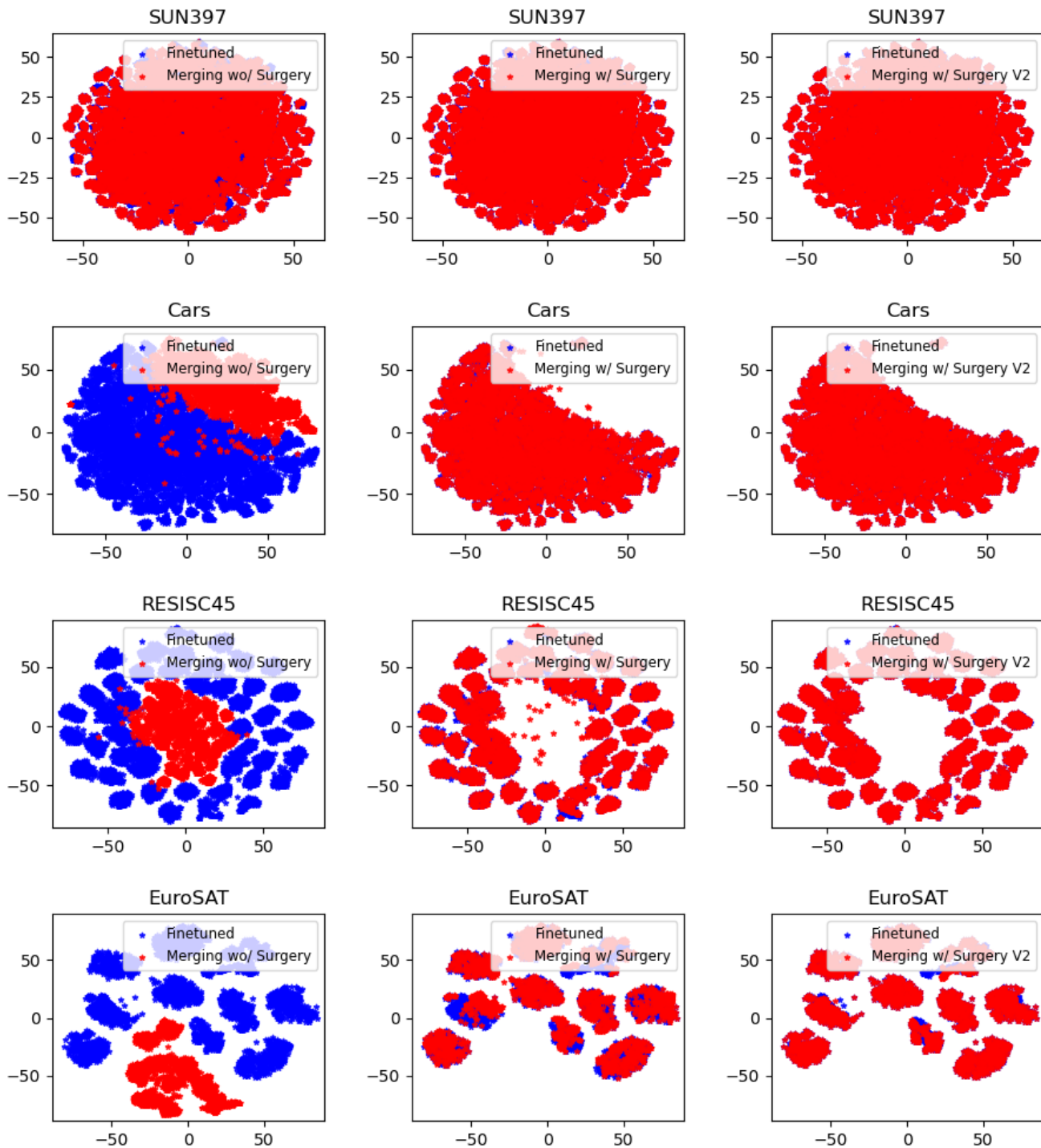


Fig. 15: Visualization of the distribution of extracted representations (final layer) for individual models (blue) and merged model (red) in the setup of ViT-B/32 architecture and Task Arithmetic method. The first column represents the merged model obtained by Task Arithmetic [36] without using the representation surgery scheme. The second column indicates the use of the Surgery scheme in §IV-B, and the third column indicates the use of the SurgeryV2 scheme proposed in §IV-D.

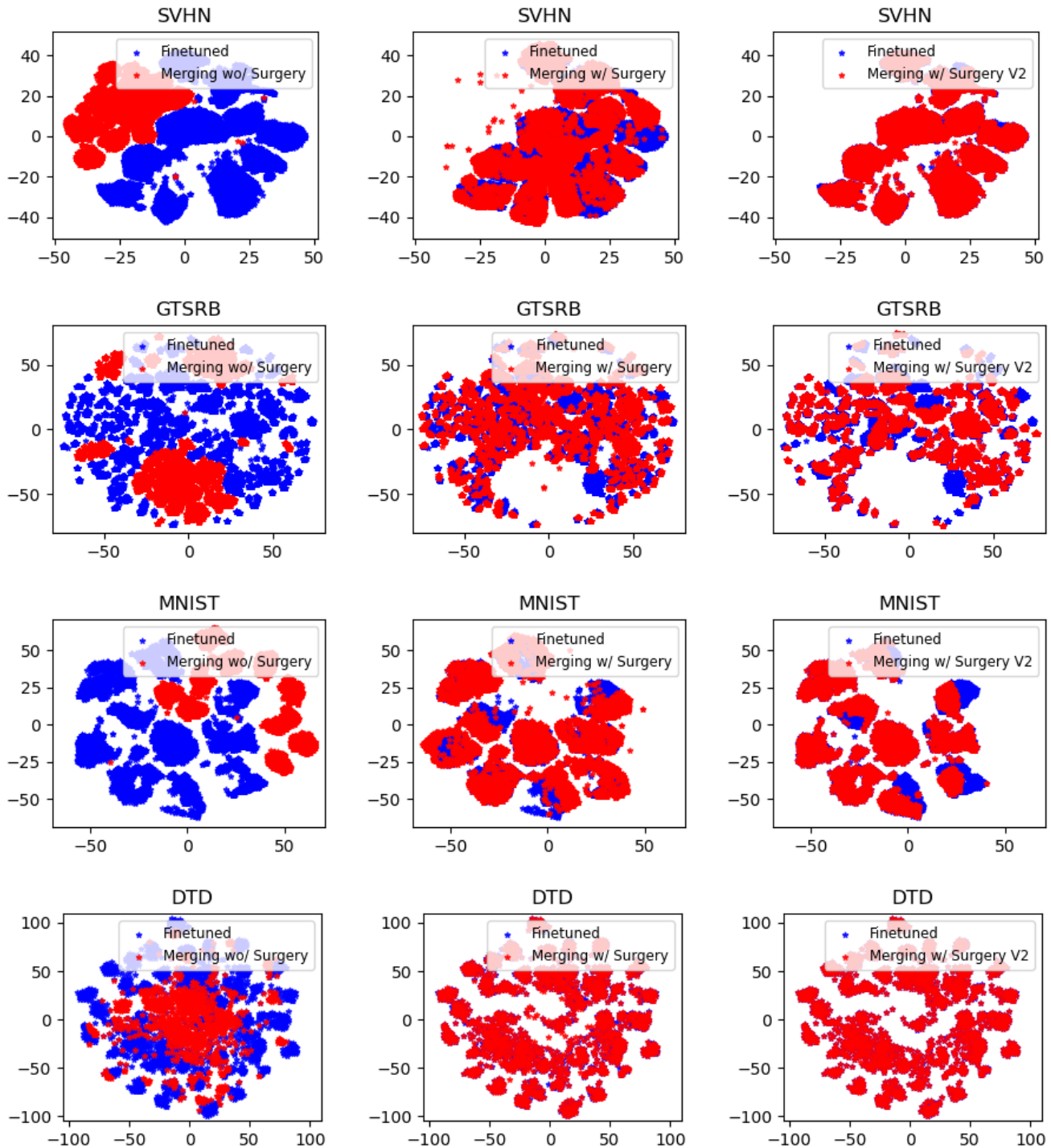


Fig. 16: Visualization of the distribution of extracted representations (final layer) for individual models (blue) and merged model (red) in the setup of ViT-B/32 architecture and Task Arithmetic method. The first column represents the merged model obtained by Task Arithmetic [36] without using the representation surgery scheme. The second column indicates the use of the Surgery scheme in §IV-B, and the third column indicates the use of the SurgeryV2 scheme proposed in §IV-D.

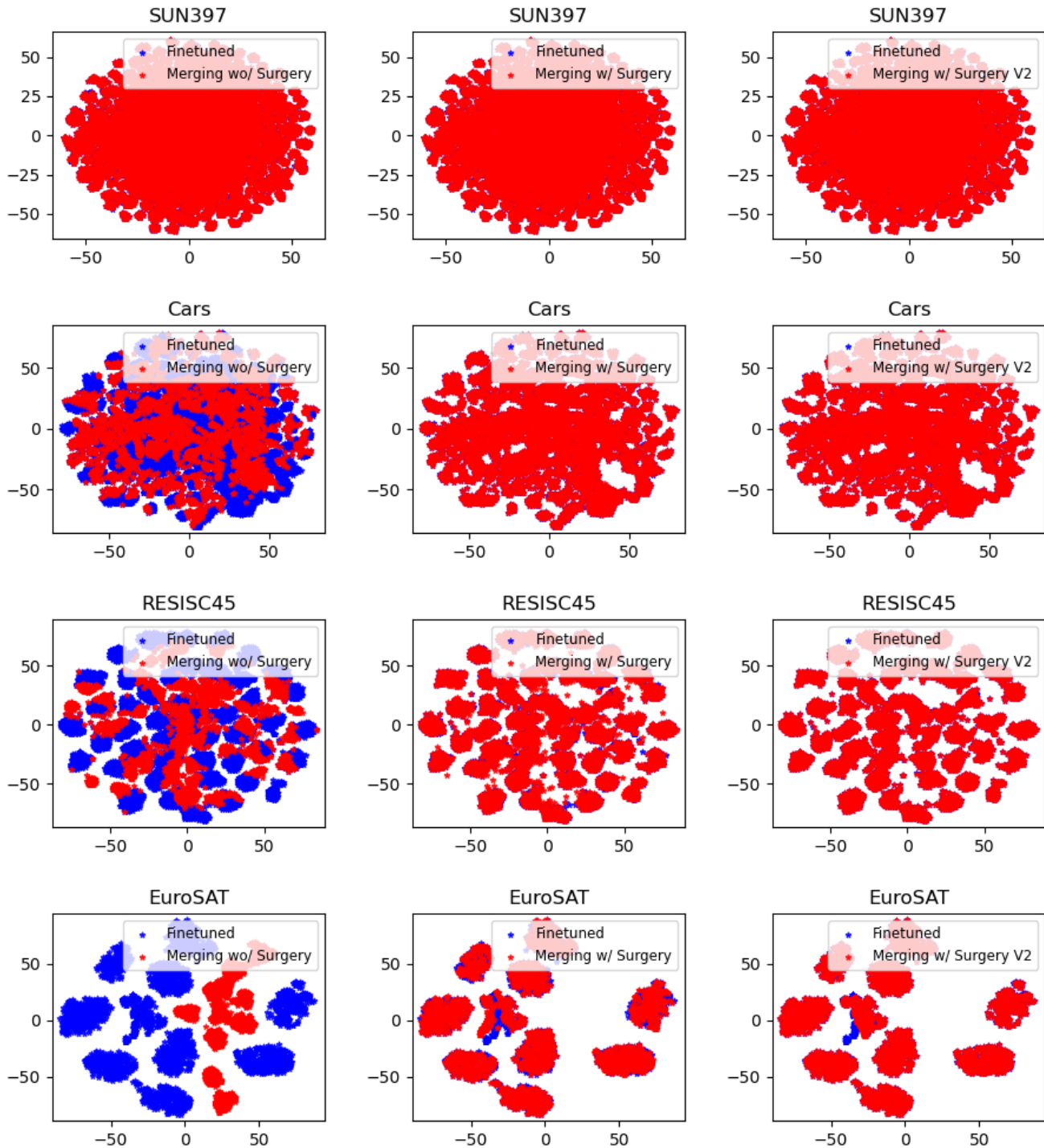


Fig. 17: Visualization of the distribution of extracted representations (final layer) for individual models (blue) and merged model (red) in the setup of **ViT-B/32 architecture and AdaMerging method**. The *first column* represents the merged model obtained by AdaMerging [26] without using the representation surgery scheme. The *second column* indicates the use of the Surgery scheme in §IV-B, and the *third column* indicates the use of the SurgeryV2 scheme proposed in §IV-D.

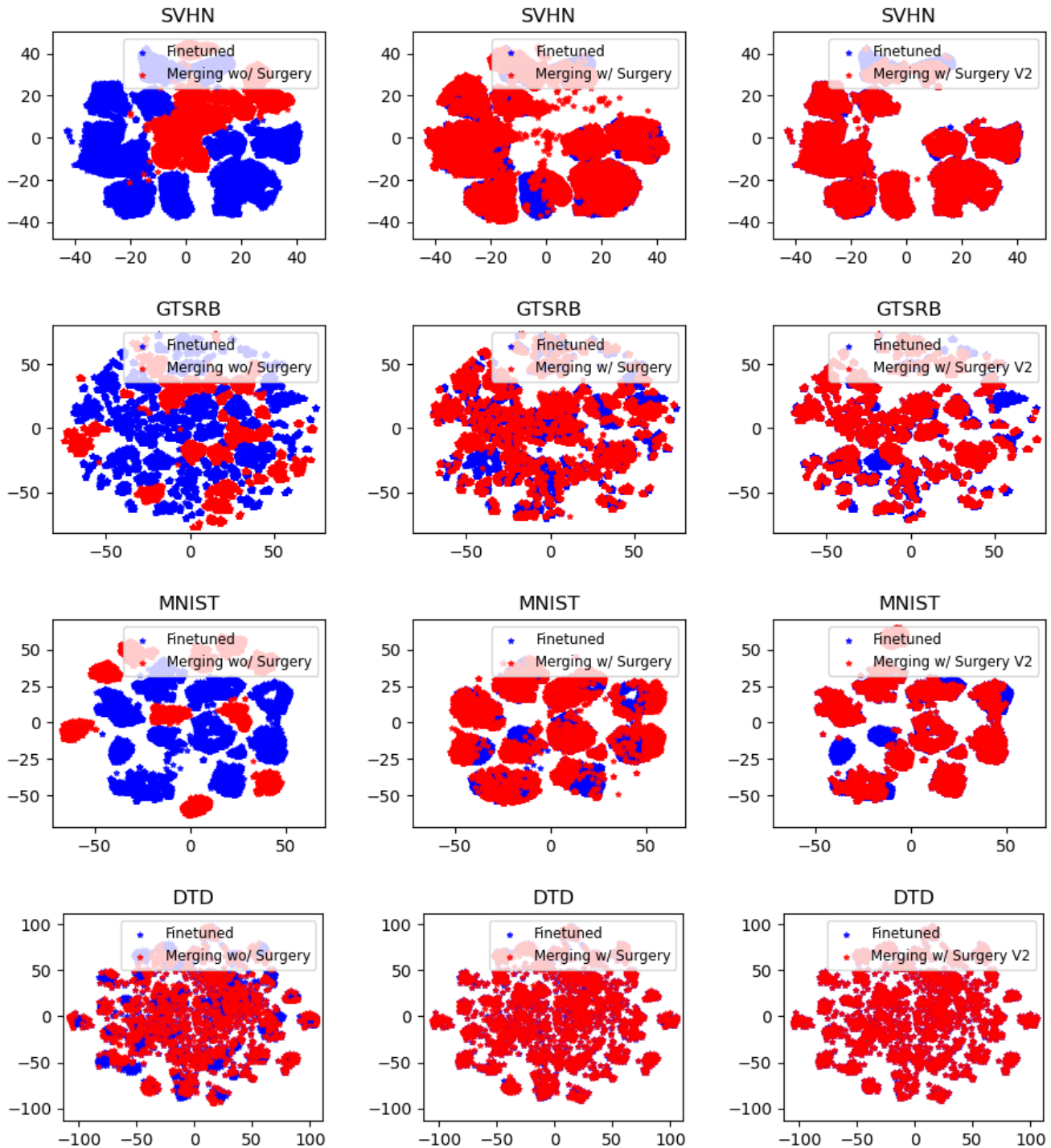


Fig. 18: Visualization of the distribution of extracted representations (final layer) for individual models (blue) and merged model (red) in the setup of **ViT-B/32 architecture and AdaMerging method**. The *first column* represents the merged model obtained by AdaMerging [26] without using the representation surgery scheme. The *second column* indicates the use of the Surgery scheme in §IV-B, and the *third column* indicates the use of the SurgeryV2 scheme proposed in §IV-D.